Strong Coupling Between Surface Plasmon Polaritons and Molecules: Lindblad Equation Approach

Master's thesis, November 9, 2016

Author:

Aili Asikainen

Supervisor:

Tero Heikkilä

UNIVERSITY OF JYVÄSKYLÄ
Department of Physics
University of Jyväskylä
November 9, 2016

Abstract

This thesis provides an introduction to strong coupling between surface plasmon polaritons (SPP) and molecules. In the strong coupling limit the energy levels of the system change to form new hybridstates. These new states can be used for example to control chemical reactions and in quantum-information technology. One property of the SPPs is that they can only be p-polarized. However, in recent experiments the strong coupling system has been found to also emit s-polarized light. One goal of this thesis is to find a process that would explain the microscopic origin of the s-polarized light. We construct a Markovian quantum master equation of the Lindblad kind for the strong coupling system. Lindblad equation is describes the time evolution of the density matrix of the system, when the system is coupled to an external bath through dissipative processes. The Lindblad equation that we construct includes decay of the SPP and molecules into an external photon field, dephasing process and inelastic scattering of the molecules with phonons. The dephasing process causes loos of interference in the system but does not change energy. Using both a numerical and an analytical treatment of the Lindblad equation we find that dephasing is not enough to produce s-polarized light. We are able to find a Lindblad term that allows the emission of s-polarised light. We argue that this term is a correction due to the finite correlation length of the external photon field.

Tiivistelmä

Pintaplasmonipolaritonit (SPP) ovat metallin ja dielektrisen aineen, esim. ilma, rajapintaan syntyviä sähkömagneettisia aaltoja. Tämä työ käsittelee SPP:en ja molekyylien välistä vuorovaikutusta vahvan kytkennän rajalla. Vahvan kytkennän rajalla systeemin energiatilat muodostavat uusia hybriditiloja. Näitä uusia tiloja voidaan hyödyntää mm. kemiallisten reaktioiden muokkaamisessa ja kvantti-informatioteknologiassa.

Eräs SPP:en ominaisuus on, että ne voivat lähettää vain p-polarisoitunutta valoa. Viimeaikaisissa tutkimuksissa on kuitenkin havaittu SPP–molekyyli-systeemin lähettävän myös s-polarisoitunutta valoa. Yksi tämän työn tavoitteista oli löytää prosessi, joka selittäisi s-polarisoituneen valon mikroskooppisen alkuperän. Tätä varten muodostin systeemille markovilaisen kvanttimekaanisen master-yhtälön Lindbladin muodossa.

Lindbladin yhtälö kuvaa systeemin tiheysmatriisin aikakehitystä, kun systeemi on kytketty ulkoiseen kylpyyn erilaisten dissipaatioprosessien myötä. Tarkastelemassani systeemissä tällaisia dissipaatioprosesseja ovat SPP:n ja molekyylien viritystilojen purkautuminen ulkoiseen fotonikenttään. Vastaavasti ulkoinen fotonikenttä voi virittää systeemin hybriditilalle. Lisäsin Lindbladin yhtälöön myös prosessin, joka sekoittaa tilan kvanttimekaanisen vaiheen. Se vähentää systeemin kvanttitilojen interferenssiä, mutta ei muuta systeemin energiaa. Tämä prosessi syntyy elastista törmäyksistä molekyylien ja metallin kidevärähtelyiden, fononien, välillä. Toisaalta molekyylit ja fononit voivat myös törmätä epäelastisesti.

Ratkaisin Lindbladin yhtälön numeerisesti kahden molekyylin tapauksessa. Numeerisen ratkaisun päätuloksena sain, että kun dissipaatioprosessit tapahtuvat riittävän hitaasti verrattuna systeemin sisäiseen kytkentään, tiheysmatriisin ei-diagonaaliset alkiot ovat niin pieniä, että ne voi jättää huomioimatta. Olettaen, että ei-diagonaali alkiot ovat pieniä, löysin Lindbladin yhtälön stationäärisen ratkaisun, kun molekyylien lukumäärä on suuri. Tämän tuloksen avulla huomasin, että muodostamani termi kvanttimekaanisen vaiheen sekoittumiselle ei luo s-polarisoitunutta valoa.

Löysin Lindbladin yhtälöön lisättävän termin, jonka seurauksena systeemi lähettää s-polarisoitunutta valoa. Esitän, että tällainen termi voi olla korjaustermi, joka johtuu fotonikentän äärellisestä korrelaatiopituudesta. Tämä korjaus näyttäisi siltä kuin molekyylit olisivat kytkeytyneet erillisiin fotonikenttiin. Ratkaisin analyyttisesti Lindbladin yhtälön, joka sisälsi korjaustermin, mutta ei vaiheen sekoittumista. Ratkaisun avulla sain suhteen eri polarisaatiosuuntiin lähetetylle valolle, tämä suhde riippuu mm. SPP:n polarisaatiosta ja dissipaatioprosessien nopeuksista.

Työssa saatujen tulosten avulla voidaan jatkaa SPP–molekyyli-systeemin teoreettisen mallin kehitystä. Tärkeää on ymmärtää tarkemmin lisätyn korjaustermi mikroskooppinen perusta, jotta mallia voi testata kokeellisesti, sekä pohtia muita mahdollisia Lindblad yhtälön termejä.

Contents

1 Introduction

Free electrons in a metal form a plasma that can sustain plasmons, collective oscillations of the electrons. These plasmons can interact with electromagnetic radiation in the surface of the metal to form surface plasmon polaritons (SPP).

Surface plasmon polaritons have many properties that allow applications that cannot be achieved with free electromagnetic radiation. They can be confined near the surface into space that is smaller than the wave length of free electromagnetic radiation with the same frequency. The electric field associated with the surface plasmon polaritons decays rapidly when going further from the surface and the electric field is enhanced adjacent to the surface.[1] The sub-wavelength property allows the use of SPPs in nano-optics. SPPs can also be used in other applications, e.g. spectroscopy and biosensing.[2] A classical introduction to the properties of surface plasmon polaritons is presented in section 2 of this thesis.

Due to the field enhancement and other properties of the surface plasmon polaritons it is possible to achieve strong coupling between them and quantum emitters. These quantum emitters can be for example dye molecules or quantum dots. Strong coupling between surface plasmon polaritons and quantum emitters has been measured even at room temperature.[1, 2]

In the strong coupling limit the energy levels of the system are changed so that new hybrid states are formed. The change in the energy levels is proportional to the strength of the coupling. The new levels correspond to hybrid superpositions of the original states. Strong coupling between cavity photons and quantum emitters has been used to modify chemical reactions[3]. Strong coupling also has applications in quantum-information technology. In section 3 we use the Jaynes-Cummings model for the surface plasmon polariton–molecule system to describe the strong coupling regime.

The strongly coupled system of surface plasmon polaritons and molecules emits light into their environment. Recently the polarization of this light has been studied experimentally.[4] The SPPs can only be p-polarized so it is not surprising that some of the emitted light is p-polarized. However it was also observed that some of the emitted light may be s-polarized.

To our knowledge currently no theoretical model exists that would explain the observation of s-polarized light. One goal of this thesis is to find a theoretical description that would allow for the emission of s-polarized light. Because emission of light into the environment plays an important role we need to employ the concepts of open quantum systems. We use the Markovian quantum master equation in the Lindblad form. It is a quantum mechanical equivalent to the classical master equation. Open quantum systems and the Lindblad equation are discussed in section 4.

The Lindblad equation approach enables us to consider different dissipation mechanisms. Firstly the quantum emitters may decay into the ground state by emitting photons, similarly the surface plasmon polaritons may decay by emitting photons. The system may also be pumped by excitation into the hybrid state.

The molecular quantum emitters have vibrational states that can have elastic or inelastic collisions with phonons. Elastic collisions do not change the average energy but instead lead to a loss of interference in the system. This is called dephasing. Inelastic collisions may cause decay of the quantum emitters.

Microscopic models for the strong coupling system involving dissipation have been recently discussed by e.g. Gonzáles-Tudela et. al. [5] and Pino et. al. [6]. Gonzáles-Tudela et. al. construct a Lindblad equation involving decay of both the quantum emitters and the surface plasmons and dephasing. Pino et. al. consider a strong coupling system of molecules and an electromagnetic cavity mode. They develop a detailed description of dephasing in the strong coupling system.

In section 5 we construct a Lindblad equation including the above mentioned dissipation mechanisms by using similar arguments to [5, 6]. We put special emphasis on obtaining the polarization dependence. In section 6 we solve the Lindblad equation numerically in the case of only 2 emitters. The numerical solution gives us tools that aid simplifying the analytical solution in section 7.

We are able to obtain the stationary solution to the Lindblad equation in the $N \to \infty$ limit. We find that pure dephasing is not enough to allow for the emission of s-polarized light. We thus add a correction term that leads to the emission of s-polarized light. The correction term is related to the fact that the correlation length of the external photon field is actually not infinite. However further discussion is needed to explain the microscopical origin of the term.

This thesis includes many figures. For most of the figures the only option was to use different colours to distinguish different parts. It is advisable to consult the online version for full colour versions of the figures.

2 Surface plasmon polaritons

Surface plasmon polaritons (SPP) are electromagnetic excitations that are confined into the interface between a metal and a dielectric material. They form when light interacts with the free electrons in the surface of the metal to form hybrid modes. In addition to SPPs there are other surface modes that form from the light-matter interaction, some such modes are surface phonon polaritons and surface exciton polaritons.

This work focuses on *propagating SPPs* that are free to propagate along the surface. There are also so called *localized SPPs* that are confined in space such as the surface of a nano-sphere.[2]

Surface plasmon polaritons have a near-field character, meaning that they are confined to sub-wavelength dimensions. The near-field character allows their use to probe nano-objects smaller than free-space wavelength of light. It also allows for strong coupling between SPPs and molecules. This coupling depends on the distance between the molecule and the SPP.[2]

This section provides a short introduction to the classical theory of SPPs. We begin with the source-free Maxwell equations and use the Drude model for the free surface electrons. We derive the dispersion relation, discuss the spatial confinement and briefly look at different excitation methods.

2.1 Classical derivation

Surface plasmon polaritons can be found as a solution to the source-free Maxwell equations in the metal–dielectric interface (see figure 2.1). The metal and the dielectric are chosen to be non-magnetic, thus the magnetic permeability for both media is $\mu = 1$. The Maxwell equations are now

$$\nabla \times \vec{H} = \frac{\epsilon}{c}\frac{\partial \vec{E}}{\partial t} \qquad \nabla \times \vec{E} = -\frac{1}{c}\frac{\partial \vec{H}}{\partial t} \tag{2.1}$$

$$\nabla \cdot \vec{H} = 0 \qquad \nabla \cdot (\epsilon \vec{E}) = 0, \tag{2.2}$$

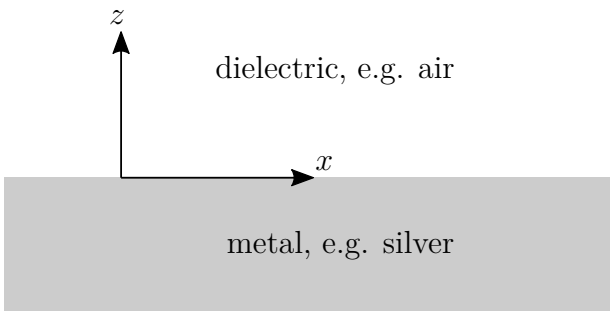

Figure 2.1: Metal dielectric interface.

where ϵ is the permittivity (or dielectric constant) of the medium. The interface sets boundary conditions for the electric and magnetic fields: [7]

- The component of the electric field parallel to the interface must be continuous, i.e.

$$\hat{n}_{md} \times (\vec{E}_m - \vec{E}_d) = 0, \tag{2.3}$$

  where m denotes the metal, d denotes the dielectric and $\hat{n}_{md}$ is the normal vector to the interface.
- The component of the magnetic field normal to the interface must be continuous, i.e.

$$\hat{n}_{md} \cdot (\vec{H}_m - \vec{H}_d) = 0. \tag{2.4}$$

- The component of the field $\epsilon\vec{E}$ normal to the interface must be continuous, i.e.

$$\hat{n}_{md} \cdot (\epsilon_m\vec{E}_m - \epsilon_d\vec{E}_d) = 0. \tag{2.5}$$

- The component of the field $\mu\vec{H}$ (or just $\vec{H}$, since $\mu = 1$), parallel to the interface must be continuous, i.e.

$$\hat{n}_{md} \times (\vec{H}_m - \vec{H}_d) = 0. \tag{2.6}$$

An electromagnetic field propagating near a surface can be divided into s- and p-polarized components. For s-polarized electromagnetic fields the electric field is perpendicular to the plane of incidence while for p-polarization the electric field is parallel to the plane of incidence. If the surface is in the $z = 0$ plane and the wave propagates into x direction, the plane of incidence is the xz-plane and the s-polarized electromagnetic field can be written as

$$\begin{aligned} \vec{E}_d &= (0, E_{d,y}, 0)\exp[i(k_{d,x}x - k_{d,z}z - \omega t)] \\ \vec{H}_d &= (H_{d,x}, 0, H_{d,z})\exp[i(k_{d,x}x - k_{d,z}z - \omega t)] \end{aligned} \tag{2.7}$$

in the dielectric ($z > 0$) and

$$\begin{aligned} \vec{E}_m &= (0, E_{m,y}, 0)\exp[i(k_{m,x}x + k_{m,z}z - \omega t)] \\ \vec{H}_m &= (H_{m,x}, 0, H_{m,z})\exp[i(k_{m,x}x + k_{m,z}z - \omega t)] \end{aligned} \tag{2.8}$$

in the metal ($z < 0$).

From the boundary conditions we get

$$E_{m,y} = E_{d,y} = E_y \quad \text{and} \quad H_{m,x} = H_{d,x} = H_x. \tag{2.9}$$

From the second equation in (2.1) and the boundary conditions we get

$$E_y(k_{m,z} + k_{d,z}) = 0. \tag{2.10}$$

Because we are looking for solutions that are confined near the surface the fields must decay in the z-direction. That means that $k_{m,z}$ and $k_{d,z}$ must both have negative imaginary parts. Equation (2.10) is now satisfied only if $E_y = 0$ and thus SPPs that are confined near the surface cannot be s-polarized.[1]

For p-polarized electromagnetic waves the electric and magnetic fields are

$$\begin{aligned}\vec{E}_d &= (E_{d,x}, 0, E_{d,z}) \exp[i(k_{d,x}x - k_{d,z}z - \omega t)] \\ \vec{H}_d &= (0, H_{d,y}, 0) \exp[i(k_{d,x}x - k_{d,z}z - \omega t)]\end{aligned} \tag{2.11}$$

in the dielectric and

$$\begin{aligned}\vec{E}_m &= (E_{m,x}, 0, E_{m,z}) \exp[i(k_{m,x}x + k_{m,z}z - \omega t)] \\ \vec{H}_m &= (0, H_{m,y}, 0) \exp[i(k_{m,x}x + k_{m,z}z - \omega t)]\end{aligned} \tag{2.12}$$

in the metal.

2.2 Dispersion relation

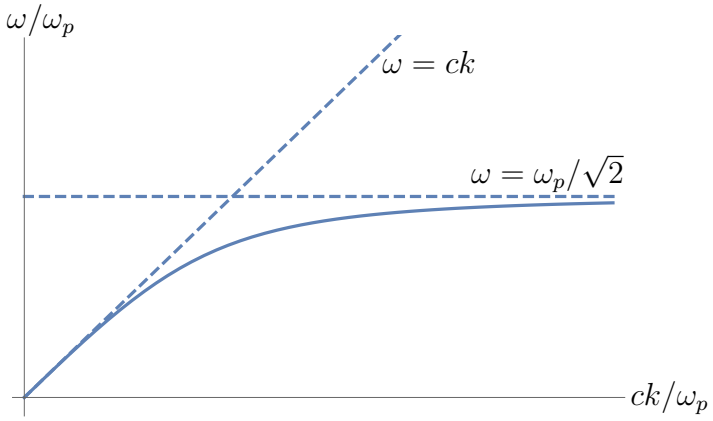

Figure 2.2: Dispersion relation for SPPs using the Drude model without losses. Plotted for $\epsilon_d = 1$, which corresponds to air. With small k the dispersion relation follows the light-line $\omega = ck$. For larger values of k the frequency approaches $\omega = \omega_p/\sqrt{2}$.

Using the relevant boundary conditions,

$$E_{m,x} = E_{d,x}, \quad B_{m,y} = B_{d,y} \quad \text{and} \quad \epsilon_m E_{m,z} = \epsilon_d E_{d,z}, \tag{2.13}$$

we can derive the dispersion relation for the in-plane wave vector

$$k_x = k_{m,x} = k_{d,x} = \frac{\omega}{c}\sqrt{\frac{\epsilon_m \epsilon_d}{\epsilon_m + \epsilon_d}}. \tag{2.14}$$

We also find that the perpendicular component of the wave vector is given by

$$k_{m/d,z}^2 = \epsilon_{m/d}\frac{\omega^2}{c^2} - k_x^2. \tag{2.15}$$

As a simple model for the electrical properties of the metal we use the Drude model. In the Drude model the permittivity of the metal is

$$\epsilon_m(\omega) = 1 - \frac{\omega_p^2}{\omega^2 + i\gamma\omega}, \tag{2.16}$$

where ω_p is the plasma frequency and γ is the damping rate due to losses. For metals the real part of the dielectric constant is negative so the Drude model in this form is valid for metals only in the low-frequency limit $\omega < \omega_p$. The Drude model is very simple and does not account for e.g. nonlocal effects, where the permittivity can also depend on the wave vector. It is however sufficient at demonstrating some of the important properties of SPPs.[1]

Using the Drude model without losses for the metal and $\epsilon_d = 1$, corresponding to air, for the dielectric, the dispersion relation becomes

$$\omega^2 = c^2 k_x^2 + \frac{\omega_p^2}{2} \pm \sqrt{c^4 k_x^4 + \frac{\omega_p^4}{4}}. \tag{2.17}$$

For the upper branch (plus sign), if $ck_x >> \omega_p$, the dispersion relation would be $\omega_+ = 2ck_x$, which corresponds to light moving at twice the speed of light. Because of that the upper branch solution is disregarded as unphysical.

The lower branch of the dispersion relation is plotted in figure 2.2. With small k_x the SPP mode behaves like free light for which $\omega = ck$. For large values of k_x the frequency asymptotically approaches the value $\omega_p/\sqrt{1+\epsilon_d}$. The dispersion relation is always below the light-line meaning that free light cannot couple to SPPs directly.[2]

2.3 Confinement

Because of the losses, caused by the imaginary part of k_x, the electric and magnetic fields decay in the propagation direction. The propagation length, or the distance that the SPP propagates before decaying by a factor of $1/e$, is

$$1/L_x = \mathrm{Im}(k_x) = \frac{\omega}{c}\mathrm{Im}\sqrt{\frac{\epsilon_m \epsilon_d}{\epsilon_m + \epsilon_d}}. \tag{2.18}$$

The decay is due to ohmic losses into the medium and the energy carried by the SPP is converted into heat.

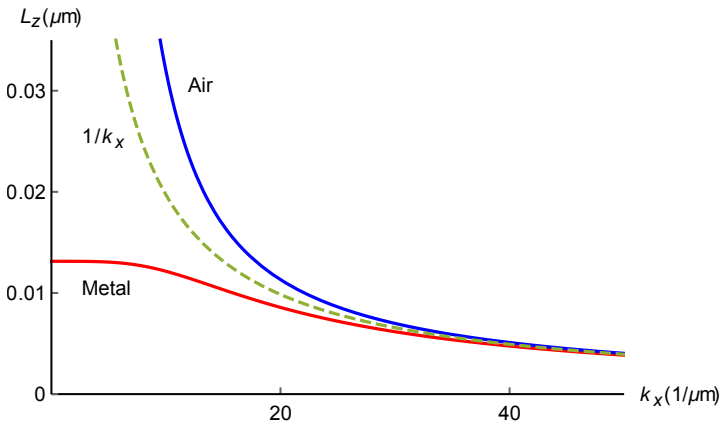

Figure 2.3: Skin depth as a function of the wave vector k_x. The plasma energy of the metal is $\omega_p = 15\,\mathrm{eV}$. The permittivity of the dielectric is set to $\epsilon_d = 1$, corresponding to air.

In addition to decay in the propagation direction the fields decay quickly in the metal and the dielectric. The decay length in the media, or the skin depth, is given by

$$1/L_{m/d} = \mathrm{Im}(k_{m/d,z}) = \frac{\omega}{c}\mathrm{Im}\sqrt{\frac{\epsilon_{m/d}^2}{\epsilon_m + \epsilon_d}}. \tag{2.19}$$

Equation (2.15) shows that $\mathrm{Im}(k_{m/d,z}) \neq 0$ even without the losses γ, if $k_x^2 > \frac{\omega^2}{c^2}\epsilon_{m/d}$. Figure 2.3 shows the skin depth as a function of the wave vector k_x. In the metal the SPP is confined to near the surface for all wave vectors. In the dielectric only SPPs with large wave vectors are confined. For large wave vectors the skin depth in both the metal and the dielectric approaches $1/k_x$. Due to the exponential decay the electric field is strongest adjacent to the surface.

2.4 Excitation

The dispersion relation for the SPP in figure 2.2 is always below the light-line which means that the frequency and wave vector of the SPP can never directly match those of free light. Because of that SPPs cannot directly couple to free light. Instead the electromagnetic field of the light has to be manipulated somehow so that it matches the wave vector and momentum of the SPP. This can be achieved for example with prisms or by grating.

When light is incident to a wall of a prism from the inside, if the angle of incidence is greater than the angle of reflection, the light is fully reflected. This reflection however does not happen entirely inside the prism. The field penetrates the surface and decays exponentially outside the prism. With a suitable refractive index the wave vector of the light can be adjusted to match the SPP. In the Otto geometry [8] the prism is placed within a wavelength of the metal surface where the light may now couple to the surface plasmons. Another configuration used is the Kretschmann geometry [8], where the prism is placed on top of a thin metal film and SPPs form on the bottom surface of the metal.

Surface roughness can cause the light to diffract in a way that changes the wave vector to match the surface plasmon mode. For example periodic grating of the surface can be used to excite SPPs.[8]

3 Strong coupling

The interaction between two systems can be roughly divided into two regimes, the weak- and the strong-coupling regime. Weak coupling is the limit of perturbation theory. In the weak-coupling regime damping is much stronger than the coupling and the effects of the coupling on the dispersion are negligible. In the case of strong coupling the coupling is stronger than damping and the energy level structure changes in a way that the systems can no longer be distinguished and they form hybrid modes. Above the SPP dispersion relation shows hints of strong coupling since the SPP mode had very different energy (frequency) compared to the light mode and the plasmon mode.

The change in the energy structure due to strong coupling can be used for example to modify chemical reactions and reaction rates. Other applications involve devices in quantum information technology.[2]

This section focuses on the strong coupling of a surface plasmon polariton and molecules (modeled by a two-state system). We use the Jaynes-Cummings Hamiltonian in the low energy limit. Important concepts of avoided crossing and vacuum Rabi splitting are discussed in this example. For later use we define the eigenstates of the strong coupling system.

3.1 Strong coupling of a SPP and molecules

Consider a system where a single surface plasmon polariton with frequency ω_p couples strongly to an ensemble of N molecules. The molecules are considered to be two-state systems with transition energy ω_m and transition dipole moments in arbitrary directions $\hat{n}_j$.

The operator algebra of a two-state system is represented by the Pauli-matrices. If the system has a ground state $|g\rangle = \left(\begin{smallmatrix}0\\1\end{smallmatrix}\right)$ and an exited state $|e\rangle = \left(\begin{smallmatrix}1\\0\end{smallmatrix}\right)$, the matrices $\sigma_\pm = 1/2(\sigma_x \pm i\sigma_y)$ induce transitions between the states, i.e. $\sigma_+|g\rangle = |e\rangle$, $\sigma_-|e\rangle = |g\rangle$. Moreover the operator $\sigma_+\sigma_-$ is the number operator for the excited states, i.e. $\sigma_+\sigma_-|g\rangle = 0$, $\sigma_+\sigma_-|e\rangle = |e\rangle$.

The Hamiltonian of the coupled system is

$$H = H_p + H_m + H_I, \tag{3.1}$$

where $H_p = \omega_p a^\dagger a$ and $H_m = \omega_m \sum_j \sigma_{+,j}\sigma_{-,j}$. Here $a^{(\dagger)}$ is the SPP annihilation (creation) operator, that follows the bosonic commutation relations, $[a, a^\dagger] = 1$, $[a^{(\dagger)}, a^{(\dagger)}] = 0$. The interaction term for a quantum electric field and a two-state system can be written in the dipole approximation [9]

$$H_I = \sum_j g_j(a + a^\dagger)(\sigma_{+,j} + \sigma_{-,j}), \tag{3.2}$$

where g_j are the coupling constants for the interaction. We assume that the coupling constants depend only on the angle between the transition dipole moment of the molecule $\hat{n}_j$ and the polarization of the SPP $\hat{u}_p$, so that $g_j = g(\hat{n}_j \cdot \hat{u}_p)$.

In the interaction picture the interaction term is

$$H_I(t) = \sum_j g_j(ae^{-i\omega_p t} + a^\dagger e^{i\omega_p t})(\sigma_{+,j}e^{-i\omega_m t} + \sigma_{-,j}e^{-i\omega_m t}). \tag{3.3}$$

If the system is close to resonance, i.e. $\omega_p \sim \omega_m$, the frequency $\omega_p + \omega_m$ is much higher than the other frequency $\omega_p - \omega_m$. We can thus make the *rotating wave approximation* that neglects all the terms with $e^{\pm i(\omega_p+\omega_m)t}$. For the rotating wave approximation to be valid the coupling g must be much smaller than ω_m. If the coupling is of the order of ω_m the system is said to be in the ultrastrong coupling regime. [2]

After the rotating wave approximation the total Hamiltonian of the system is in the Shrödinger picture

$$H = \omega_p a^\dagger a + \omega_m \sum_j \sigma_{+,j}\sigma_{-,j} + \sum_j g_j(\sigma_{+,j}a + \sigma_{-,j}a^\dagger). \tag{3.4}$$

This is the Jaynes-Cummings Hamiltonian with many molecules. Its spectrum can be solved exactly [10], but we simplify the treatment by taking the low energy limit.

3.2 Eigenenergies and eigenstates

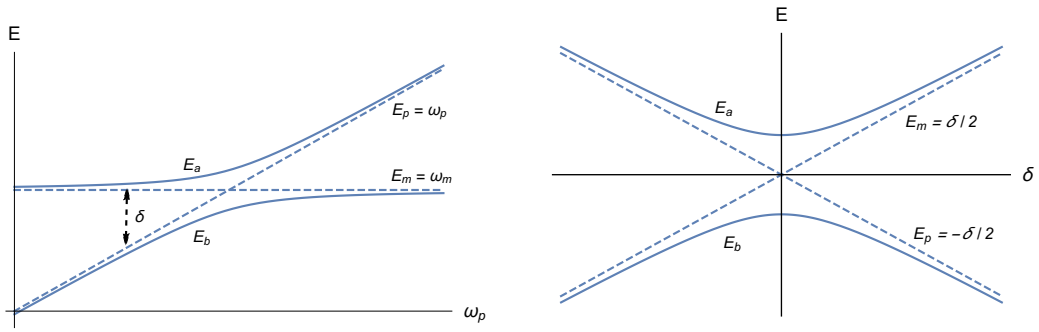

(a) Avoided crossing

(b) Avoided crossing in a frame that rotates with frequency $\frac{\omega_m+\omega_p}{2}$

Figure 3.1: Energy levels of the strongly coupled system. The dashed lines are the energies of the plasmon and molecules in the uncoupled system. When the coupling is turned on the system forms new eigenstates. Far from resonance, $|\delta|$ large, the system behaves as the uncoupled system. Near resonance, $|\delta|$ small, the energy levels change into an *avoided crossing* due to the strong coupling.

In the low energy limit we assume that only one molecule or SPP can be excited at a time. The N particle system has then $N + 2$ possible states: the vacuum, where there is no SPP and all N molecules are in the ground state $|0\rangle = |0g_1 \dots g_N\rangle$, the N states where a single molecule has been excited $|j\rangle = |0g_1 \dots e_j \dots g_N\rangle$ and the state with a single SPP $|p\rangle = |1g_1 \dots g_N\rangle$.

In terms of these states the Hamiltonian is

$$H = 0|0\rangle\langle 0| + \omega_p|p\rangle\langle p| + \omega_m \sum_{j=1}^{N} |j\rangle\langle j| + g\sum_{j=1}^{N}(\hat{n}_j \cdot \hat{u}_p)(|j\rangle\langle p| + |p\rangle\langle j|). \tag{3.5}$$

Since this Hamiltonian is $(N+2)\times(N+2)$ dimensional it has $N+2$ eigenstates.

The first eigenstate is the vacuum state $|0\rangle$ with energy $E_0 = 0$. There are also $N-1$ eigenstates with only molecule excitations all with energy $E_m = \omega_m$. These states are superpositions of the molecule states $|j\rangle$

$$|m\rangle = \sum_{j=1}^{N} \eta_{mj}|j\rangle, \tag{3.6}$$

where η_{mj} need to be determined later. The final two states are coupled states between the SPP and the molecules with energies

$$E_{b/a} = \frac{\omega_p + \omega_m}{2} \mp \frac{\omega_g}{2}, \tag{3.7}$$

where $\omega_g = \sqrt{4g^2\sum_j(\hat{n}_j\cdot\hat{u}_p)^2 + \delta^2}$ and $\delta = \omega_m - \omega_p$. The bonding and antibonding states are

$$|b/a\rangle = \frac{-\delta \mp \omega_g}{\sqrt{2\omega_g(\omega_g \pm \delta)}}|p\rangle + \frac{\sqrt{2}}{\sqrt{\omega_g(\omega_g\pm\delta)}}\sum_j g_j|j\rangle = \alpha_{b/a}|p\rangle + \beta_{b/a}\sum_j g_j|j\rangle. \tag{3.8}$$

The coupling produces an *avoided crossing* in the energy levels as in figure 3.1. Far from resonance, when $|\delta|$ is large, the coupled system behaves like the free system. However near resonance, when $|\delta|$ is small, the coupling changes the energy levels so that they no longer cross. The difference between the energies of the bonding and antibonding states depends on the strength of the coupling. At resonance the splitting of the bonding and antibonding energies is $\Omega = E_a(\delta=0) - E_b(\delta=0) = 2g\sqrt{\sum_j(\hat{n_j}\cdot\hat{u_p})^2}$. One definition for the strong coupling regime is that the system is strongly coupled when this splitting, called *vacuum Rabi splitting*, can be observed experimentally.[2]

Changing into a frame that is rotating with frequency $\frac{\omega_m+\omega_p}{2}$ does not change the eigenstates, but the new shifted eigenenergies are:

$$E_0 = -\frac{\omega_m+\omega_p}{2}, \quad E_{b/a} = \mp\frac{\omega_g}{2} \quad \text{and} \quad E_m = \frac{\delta}{2}. \tag{3.9}$$

Figure 3.1b shows the energy levels in this frame. Since $\omega_g = \sqrt{4g^2\sum_j(\hat{n_j}\cdot\hat{u_p}) + \delta^2} > \delta$ the states are ordered so that the molecule superposition states $|m\rangle$ are always between the hybrid bonding and antibonding states $|b/a\rangle$ in energy. Below the bonding state in energy is the vacuum state.

3.3 Molecule superposition states

We still need to fully define the molecule superposition states $|m\rangle$. Since the eigenbasis has to be orthonormal we have restrictions for the η_{mj} coefficients in equation (3.6). The molecule states need to be orthogonal to the bonding and antibonding states

$$0 = \langle a|m\rangle = \beta_a\sum_j g_j\eta_{mj} \tag{3.10}$$

and orthonormal to each other

$$\delta_{mn} = \langle m|n\rangle = \sum_j \eta^*_{mj}\eta_{nj}. \tag{3.11}$$

If the number of molecules is N there are $N-1$ molecule states $|m\rangle$ and $(N-1)\times N$ unknown coefficients η_{mj}. The orthonormality conditions (3.10) and (3.11) provide $2(N-1)$ independent equations for the coefficients. As the number of molecules increases so does the number of degrees of freedom for the coefficients also. Thus we do not provide an analytical form for the coefficients for N molecules, instead as an example we look at the $N=2$ case and for later purposes the $N\to\infty$ case.

We assumed that the molecules are arranged so that their transition dipole moments $\hat{n}_j$ are evenly distributed to all directions. For a finite number of molecules we assume that the angle between the transition dipole moment of the jth molecule and the polarization of the SPP is

$$\hat{n}_j \cdot \hat{u}_p = \cos(\theta_j), \tag{3.12}$$

where $\theta_j = \frac{\pi(j-1)}{N-1}$.

For the $N=2$ case there is only one molecule superposition eigenstate

$$|m_1\rangle = \eta_{11}|j_1\rangle + \eta_{12}|j_2\rangle \tag{3.13}$$

and only two undefined coefficients. We also have two equations from the orthonormality condition

$$\begin{aligned} &g_1\eta_{11} + g_2\eta_{12} = g(\cos(0)\eta_{11} + \cos(\pi)\eta_{12}) = 0 \\ &\eta^*_{11}\eta_{11} + \eta^*_{12}\eta_{12} = 1 \end{aligned} \tag{3.14}$$

and the system should be fully defined. The system of equations is satisfied by $\eta_{11} = \eta_{12} = \frac{1}{\sqrt{2}}$ and the molecule superposition eigenstate is

$$|m_1\rangle = \frac{1}{\sqrt{2}}(|j_1\rangle + |j_2\rangle). \tag{3.15}$$

In the $N\to\infty$ case we can go from the discrete j sum into a continuous integral in the spherical coordinates

$$\sum_j \to \frac{N}{4\pi}\int_0^{2\pi} \mathrm{d}\phi_j \int_0^{\pi} \mathrm{d}\theta_j \sin(\theta_j). \tag{3.16}$$

Now instead of discrete coefficients we are looking for functions. One choice for functions that satisfy the orthonormality conditions are the *spherical harmonics*

$$\eta_{mj} = \frac{1}{\sqrt{N}} Y^0_m(\theta_j, \phi_j) = \frac{1}{\sqrt{N}}\sqrt{2m+1}P_m(\cos\theta_j), \tag{3.17}$$

where $P_m(x)$ are the Legendre polynomials (see Appendix A for definition and properties). Since these functions need to be orthogonal to $g_j = g\cos\theta_j$, we cannot use the first Legendre polynomial $P_1(\cos\theta) = \cos\theta$. Thus we define that m takes values from the set $\{0, 2, 3, \ldots, N-1\}$.

3.4 Transformation into the eigenbasis

In this section we define the transformation from the natural $\{|0\rangle, |p\rangle, |j\rangle\}$ basis into the eigenbasis $\{|0\rangle, |a\rangle, |b\rangle, |m\rangle\}$. Firstly in the eigenbasis the Hamiltonian can be written as

$$H = E_0|0\rangle\langle 0| + E_m \sum_{n=1}^{N-1} |m_n\rangle\langle m_n| + E_a|a\rangle\langle a| + E_b|b\rangle\langle b|. \tag{3.18}$$

The original states $|p\rangle$ and $|j\rangle$ can be written in terms of the eigenstates as

$$\begin{aligned} |p\rangle &= \gamma_a|a\rangle + \gamma_b|b\rangle = \frac{1}{\sqrt{2\omega_g}}(\sqrt{\omega_g - \delta}|a\rangle - \sqrt{\omega_g + \delta}|b\rangle) \\ |j\rangle &= \sum_h \epsilon_{jh}|h\rangle = \epsilon_j|a\rangle + \xi_j|b\rangle + \sum_m \nu_{jm}|m\rangle, \end{aligned} \tag{3.19}$$

where the coefficients ϵ_j,ξ_j and ν_{jm} are obey equations

$$\begin{aligned} &\epsilon_j\alpha_a + \xi_j\alpha_b = 0 \\ &(\epsilon_j\beta_a + \xi_j\beta_b)g_k + \sum_m \nu_{jm}\eta_{mk} = \delta_{jk}. \end{aligned} \tag{3.20}$$

Multiplying the second equation in (3.20) with η^*_{nk}, summing over k and using the orthonormality relations we notice $\nu_{jn} = \eta^*_{nj}$. Similarly multiplying with ν^*_{jn} and summing over j, we find $\sum_j \xi_j\nu^*_{jn} = 0$. Multiplying with ξ_j and summing over j and using the results obtained above, we get

$$\begin{aligned} \epsilon_j &= \frac{\sqrt{\omega_g + \delta}}{\sqrt{2\omega_g}} \frac{g_j}{\sqrt{\sum_l g_l^2}} \\ \xi_j &= \frac{\sqrt{\omega_g - \delta}}{\sqrt{2\omega_g}} \frac{g_j}{\sqrt{\sum_l g_l^2}}. \end{aligned} \tag{3.21}$$

Plugging the coefficients into the second equation in (3.20) we obtain a useful formula for the sum of the molecule coefficients η_{mj}

$$\sum_m \eta^*_{mj}\eta_{mk} = \delta_{jk} - \frac{g_j g_k}{\sum_l g_l^2}. \tag{3.22}$$

Now the only unknowns in the eigenbasis representation are the coefficients η_{mj}, which can be chosen as in section 3.3. We use this transformation in sections 6 and 7 to transform the Lindblad equation into the energy eigenbasis.

4 Open quantum systems

Unlike often is assumed, no physical system is truly isolated or closed. Instead, there is always some environment that the system interacts with. Often the interaction is small enough that the environment can be neglected, but especially with quantum systems the interaction may cause relevant phenomena in the system.

Usually in open quantum systems the environment is assumed to be some kind of an infinite bath or reservoir. The environment can then cause stochastic effects in the system like dissipation and dephasing. Open quantum systems are generally very complicated because of limited knowledge of the environment. To simplify the treatment two assumptions are usually made, the Born approximation and the Markov apprximation.

In this section we define the density operator, a very useful tool for open quantum systems. We discuss pure and mixed states and the reduced density operator. The second part of this section is dedicated to finding the time evolution of the reduced density operator, or the quantum master equation of the Lindblad form.

4.1 Density matrix

Quantum systems are often described by a state vector from which one can calculate probabilities of finding the system in a given state after a measurement. This description is enough if we know with certainty that the system was in a given state at a given time. However if the system is stochastic, i.e. there are a number of possible states the system could randomly choose from at a given time, the state vector is no longer sufficient in describing the system.

A more suitable tool is the density operator. If the system is in state $|\psi_i\rangle$ $(i = 1, 2, 3 \ldots)$ with probability p_i ($p_i \in [0, 1]$,$\sum_i p_i = 1$) we define the density operator as [11]

$$\rho = \sum_i p_i |\psi_i\rangle\langle\psi_i|. \tag{4.1}$$

Note that the states $|\psi_i\rangle$ do not have to be orthonormal. If we choose an orthonormal basis $|\phi_n\rangle$, the states $|\psi_i\rangle$ can be written as the superposition of the basis states $|\psi_i\rangle = \sum_n a_n^i |\phi_n\rangle$, where a_n^i are complex constants. In this basis the density operator can be represented by a matrix with matrix elements

$$\langle\phi_n|\rho|\phi_m\rangle = \sum_i p_i a_n^i a_m^{i*}. \tag{4.2}$$

It is not hard to prove that the density operator,

1. is Hermitian, i.e. $\rho^\dagger = \rho$,
2. has unit trace, i.e. $\mathrm{Tr}(\rho) = 1$,
3. and is positive semi-definite, i.e. $\langle\phi|\rho|\phi\rangle \geq 0$ for all states $|\phi\rangle$.

Because of these properties the density matrix is diagonizable and has real, non-negative eigenvalues. Due to the trace condition the eigenvalues sum to one. Thus the eigenvalues

are probabilities. The density operator offers a practical way of calculating expectation values of operators

$$\begin{aligned}\langle A\rangle &= \sum_i p_i \langle\psi_i|A|\psi_i\rangle = \sum_{nm}\sum_i p_i a_n^i a_m^{i*}\langle\phi_m|A|\phi_n\rangle \\ &= \sum_n \langle\phi_n|\rho\sum_m |\phi_m\rangle\langle\phi_m|A|\phi_n\rangle = \sum_n \langle\phi_n|\rho A|\phi_n\rangle \\ &= \mathrm{Tr}(\rho A),\end{aligned} \tag{4.3}$$

where we have made the transformation into the orthonormal basis and used equation (4.2).

4.1.1 Pure and mixed states

A density operator that is described by only one state vector is called pure and the system is in a *pure state*. A system with a pure density operator [11]

$$\rho = |\psi\rangle\langle\psi| \tag{4.4}$$

is with certainty in the state $|\psi\rangle$. In any representation a system is in a pure state if and only if $\rho^2 = \rho$. From this it follows that for a pure density operator $\mathrm{Tr}(\rho^2) = 1$.

The traditional state vector representation is sufficient for systems that stay in a pure state. A statistical ensemble of pure states is a *mixed state*. Mixed states cannot be represented by only one state vector and they arise from the lack of knowledge of the exact state of the system. For example for a thermal bath in equilibrium, the probability of finding the system in state $|\psi_i\rangle$ with energy E_i is $p_i = e^{-\beta E_i}/\mathcal{Z}$, and the density matrix is [12]

$$\rho = \sum_i \frac{e^{-\beta E_i}}{\mathcal{Z}}|\psi_i\rangle\langle\psi_i| = \frac{e^{-\beta H}}{\mathcal{Z}}, \tag{4.5}$$

where H is the Hamiltonian operator ($H|\psi_i\rangle = E_i|\psi_i\rangle$) and $\mathcal{Z} = \mathrm{Tr}(e^{-\beta H})$. The density matrix is pure only at $\beta \to \infty$, because we do not consider the exact state of all of the particles in the bath. Instead we chose to look at the bath as a statistical ensemble and disregarded information about the exact microstates. The density matrix (4.5) is more correctly a *reduced density matrix* that we discuss in section 4.1.3.

4.1.2 Time-evolution in the interaction picture

If the Hamiltonian operator of the system in Schrödinger picture is $H = H_0 + V$, then the time evolution of the states in the interaction picture is given by ($\hbar = 1$)

$$i\frac{\mathrm{d}}{\mathrm{d}t}|\psi_i(t)\rangle = V(t)|\psi_i(t)\rangle, \tag{4.6}$$

where $V(t) = e^{iH_0 t}Ve^{-iH_0 t}$. Using equation (4.6) the time-evolution of the density matrix becomes

$$\begin{aligned}i\frac{\mathrm{d}\rho(t)}{\mathrm{d}t} &= \sum_i p_i \left(i\hbar\frac{\mathrm{d}}{\mathrm{d}t}|\psi_i(t)\rangle\langle\psi_i(t)| + |\psi_i(t)\rangle i\hbar\frac{\mathrm{d}}{\mathrm{d}t}\langle\psi_i(t)|\right) \\ &= \sum_i p_i \left(V(t)|\psi_i(t)\rangle\langle\psi_i(t)| - |\psi_i(t)\rangle\langle\psi_i(t)|V(t)\right) \\ &= V(t)\rho(t) - \rho(t)V(t) = [V(t), \rho(t)].\end{aligned} \tag{4.7}$$

Equation (4.7) is known as the Liouville-von Neumann equation in the interaction picture. [11] The solution is $\rho(t) = U_I(t, t_0)\rho(t_0)U_I^\dagger(t, t_0)$, where the time-evolution operator is

$$U_I(t, t_0) = \mathcal{T}\exp\left[i\int_{t_0}^{t} \mathrm{d}t' V(t')\right]. \tag{4.8}$$

Here $\mathcal{T}$ is the time ordering operator. The time-evolution operator is unitary so the Liouville-von Neumann equation describes the unitary time evolution of the density matrix.

4.1.3 Reduced density operator

Open quantum systems compose of two parts, the interesting subsystem and the environment. Because no system is truly isolated, the environment needs to be taken into consideration. Since it is not practical to consider the whole universe, the exact state of the environment is left unkown. That produces stochastic elements into the subsystem and makes the density matrix approach useful.

Consider two coupled systems A and B. Generally the total system is in a coupled mixed state ρ_{AB}. If the two systems are independent the density matrix factorizes into $\rho_{AB} = \rho_A \otimes \rho_B$. If system B is the environment that we cannot measure directly we have to average out the exact microstate information of the system B. This can be done by taking a *partial trace* over the system B

$$\rho^A = \mathrm{Tr}_B(\rho_{AB}) = \sum_i \langle\psi_i^B|\rho_{AB}|\psi_i^B\rangle, \tag{4.9}$$

where ρ^A is the *reduced density operator* operating in the subsystem A and the states $|\psi_i^B\rangle$ are states in the subsystem B. Unless the systems are independent and pure the reduced density operator represents a mixed state.[11]

The reduced density operator follows the three rules for density operators listed above. However it generally does not follow the Liouville-von Neumann equation. In other words the time evolution of a reduced density matrix is not unitary. The elimination of the environment causes the subsystem to behave irreversibly due to the statistical way we treat the environment. Next we will find a model for the time evolution of the reduced density matrix.

4.2 Lindblad equation

In this section we derive the general form of the Lindblad equation. We mostly follow the simple outline presented by Brasil et al. [13] with some generalizations. A little more rigorous and thorough derivation using projection operators can be found in [14].

Consider a system S connected to a reservoir R. The Hamiltonian of the total system is

$$H_T = H_S \otimes 1_R + 1_S \otimes H_R + V, \tag{4.10}$$

where H_S operates in the subspace containing the system, H_R operates only in the reservoir and V is an interaction between the reservoir and the system.

In the interaction picture the interaction term is ($\hbar = 1$)

$$V(t) = \mathrm{e}^{i(H_S+H_R)t} V \mathrm{e}^{-i(H_S+H_R)t} \tag{4.11}$$

and the density matrix of the total system is

$$\rho_T(t) = \mathrm{e}^{i(H_S+H_R)t} \rho_{SR}(t) \mathrm{e}^{-i(H_S+H_R)t}, \tag{4.12}$$

where $\rho_{SR}(t)$ is the density matrix of the complete system in the Schrödinger picture. The time evolution of the total density matrix is given by the Liouville-von Neumann equation in the interaction picture

$$\frac{\mathrm{d}\rho_T(t)}{\mathrm{d}t} = -i[V(t), \rho_T(t)]. \tag{4.13}$$

By integrating equation (4.13) we get

$$\rho_T(t) = \rho_T(0) - i \int_0^t \mathrm{d}t' [V(t'), \rho_T(t')]. \tag{4.14}$$

Equation (4.14) can be substituted into the right hand side of equation (4.13)

$$\frac{\mathrm{d}\rho_T}{\mathrm{d}t} = -i[V(t), \rho_T(0)] - [V(t), \int_0^t \mathrm{d}t' [V(t'), \rho_T(t')]]. \tag{4.15}$$

Since we are not interested in the reservoir we would like to find an equation for the reduced density matrix of the subsystem, which is found by taking the partial trace over the reservoir $\rho_S(t) = \mathrm{Tr}_R\{\rho_T(t)\}$. Taking the trace we get

$$\frac{\mathrm{d}\rho_S}{\mathrm{d}t} = -i\mathrm{Tr}_R[V(t), \rho_T(0)] - \mathrm{Tr}_R[V(t), \int_0^t \mathrm{d}t' [V(t'), \rho_T(t')]. \tag{4.16}$$

So far we have not made any approximations. In the next section we make the Born and Markov approximations to obtain a Markovian quantum master equation in the weak interaction limit.

4.2.1 Approximations

Let us assume that at time $t = 0$ the system and the reservoir were independent and uncorrelated, so that $\rho_T(0) = \rho_S(0) \otimes \rho_R(0)$. This means that we choose to turn on the interaction later than $t = 0$. Now the first term on the right hand side of equation (4.16) disappears since the initial time $t = 0$ can always be chosen so that $\mathrm{Tr}_R[V(t)\rho_R(0)] = \langle V(t) \rangle_R = 0$.

Next we make the *Born approximation*. We assume that the interaction between the system and the reservoir is weak enough that the correlation between them can be disregarded in the second order. Thus at time t later than 0 the total density matrix is $\rho_T(t) \approx \rho_S(t) \otimes \rho_R(t)$. We also assume that the relaxation time τ_R of the reservoir is small enough for it to effectively stay in a stationary state during the observation timescale t, i.e. $\rho_R(t) \approx \rho_R$, when $t \gg \tau_R$.[11, 13]

In equilibrium the reservoir density operator is of the form of equation (4.5). Since the density operator of the reservoir is (approximately) stationary it must (approximately) commute with the reservoir Hamiltonian, $[H_R, \rho_R] = 0$.

In equation (4.16) $\rho_S(t)$ depends on all the earlier times $\rho_S(t')$. We can, however, assume that the state of the system at time t depends only on the state just before t, which makes the system *Markovian*. The Markovian approximation is satisfied when the time scale at which the system evolves, τ_S, is much larger than the observation time scale t.

With these approximations we can in equation (4.16) replace $\rho_S(t')$ with $\rho_S(t)$ and change the integration variable from t' to $\tau = t - t'$. We can also assume that a long time has passed after the initial time $t = 0$ and take the upper limit to infinity

$$\frac{\mathrm{d}\rho_S}{\mathrm{d}t} = -\int_0^\infty \mathrm{d}\tau \mathrm{Tr}_R[V_{SR}(t), [V_{SR}(t-\tau), \rho_S(t) \otimes \rho_R]]. \tag{4.17}$$

Equation (4.17) is called the Born-Markov equation after the two approximations made. Next we make some more simplifying assumptions about the system and the reservoir.

4.2.2 System-reservoir interaction

Let us now consider the case where the interaction is of the form

$$V_{SR} = \sum_k (S_k^\dagger \otimes R_k + S_k \otimes R_k^\dagger), \tag{4.18}$$

where S_k operates only in the subspace of the system and R_k operates in the reservoir subsystem. This kind of interactions are relevant for example when an excitation decays into the reservoir or the reservoir can excite the system. In that case S_k contains the annihilation operators for the system and R_k contains the annihilation operators for the reservoir.

To simplify the calculation we assume that $H_S = \sum_k \epsilon_k S_k^\dagger S_k$, so that $[H_S, S_k] = -\epsilon_k S_k$. Now S_k in the interaction picture is

$$S_k(t) = e^{iH_S t} S_k e^{-iH_S t} = S_k e^{-i\epsilon_k t}. \tag{4.19}$$

We also take the reservoir to be a bath of bosons for which $H_R = \sum_{k\mu} \omega_{Rk\mu} a_{k\mu}^\dagger a_{k\mu}$, where $a_{k\mu}$ and $a_{k\mu}^\dagger$ are the annihilation and creation operators in the reservoir. For the boson bath $R_k = \sum_\mu g_{k\mu} a_{k\mu}$, where $g_{k\mu}$ are the coupling constants for the system-bath interaction. In the interaction picture

$$R_k(t) = e^{iH_R t} R_k e^{-iH_R t} = \sum_\mu g_{k\mu} a_{k\mu} e^{-i\omega_{Rk\mu} t}. \tag{4.20}$$

Inserting the interaction into equation (4.17) gives

$$\begin{aligned}\frac{\mathrm{d}\rho_S}{\mathrm{d}t} = -\sum_{kl}\Big[&(S_kS_l^\dagger\rho_S(t) - S_l^\dagger\rho_S(t)S_k)\mathrm{e}^{i(\epsilon_k-\epsilon_l)t}\int_0^\infty \mathrm{d}\tau\mathrm{e}^{i\epsilon_l\tau}\mathrm{Tr}_R(R_k^\dagger(t)R_l(t-\tau)\rho_R)\\ &+(\rho_S(t)S_l^\dagger S_k - S_k\rho_S(t)S_l^\dagger)\mathrm{e}^{i(\epsilon_k-\epsilon_l)t}\int_0^\infty \mathrm{d}\tau\mathrm{e}^{i\epsilon_l\tau}\mathrm{Tr}_R(R_l(t-\tau)R_k^\dagger(t)\rho_R)\\ &+(S_k^\dagger S_l\rho_S(t) - S_l\rho_S(t)S_k^\dagger)\mathrm{e}^{-i(\epsilon_k-\epsilon_l)t}\int_0^\infty \mathrm{d}\tau\mathrm{e}^{-i\epsilon_l\tau}\mathrm{Tr}_R(R_k(t)R_l^\dagger(t-\tau)\rho_R)\\ &+(\rho_S(t)S_lS_k^\dagger - S_k^\dagger\rho_S(t)S_l)\mathrm{e}^{-i(\epsilon_k-\epsilon_l)t}\int_0^\infty \mathrm{d}\tau\mathrm{e}^{-i\epsilon_l\tau}\mathrm{Tr}_R(R_l^\dagger(t-\tau)R_k(t)\rho_R)\Big].\end{aligned} \tag{4.21}$$

The terms containing $\mathrm{Tr}_R(R_k(t)R_l(t')\rho_R)$ and $\mathrm{Tr}_R(R_k^\dagger(t)R_l^\dagger(t')\rho_R)$ have been omitted in equation (4.21) because they have an oscillatory time dependence $e^{\pm i(\epsilon_k+\epsilon_l)t}$. In the long time limit these terms vanish. There are two ways of getting nonzero contributions from the other terms. If the system states are not degenerate, i.e., $\epsilon_k \neq \epsilon_l$, only the terms where $k = l$ remain. If there are degenerate states in the system, some of the $k \neq l$ terms remain. In general we can limit the l sum to only the states where $l = k$ or $\epsilon_l = \epsilon_k$, denoted by $\sum_{k=l,\epsilon_l=\epsilon_k}$.

Since the reservoir is in a stationary state the reservoir correlators do not depend on time t, i.e., $\mathrm{Tr}_R(R_k(t)R_l^\dagger(t-t_1)\rho_R) = \mathrm{Tr}_R(R_k(t_1)R_l^\dagger(0)\rho_R)$. We define reservoir correlators in the frequency space as the Fourier transform of the time correlators

$$\begin{aligned}F_{kl}(\omega) &= \int \mathrm{d}t_1\mathrm{e}^{i\omega t_1}\mathrm{Tr}_R(R_k(0)R_l^\dagger(t_1)\rho_R)\\ F_{kl}^*(\omega) &= \int \mathrm{d}t_1\mathrm{e}^{-i\omega t_1}\mathrm{Tr}_R(R_l(t_1)R_k^\dagger(0)\rho_R)\\ G_{kl}(\omega) &= \int \mathrm{d}t_1\mathrm{e}^{i\omega t_1}\mathrm{Tr}_R(R_l^\dagger(t_1)R_k(0)\rho_R)\\ G_{kl}^*(\omega) &= \int \mathrm{d}t_1\mathrm{e}^{-i\omega t_1}\mathrm{Tr}_R(R_k^\dagger(0)R_l(t_1)\rho_R).\end{aligned} \tag{4.22}$$

In the stationary state the correlators have the symmetry $F_{kl}(\omega) = F_{lk}^*(\omega)$ and $G_{kl}(\omega) = G_{lk}^*(\omega)$.

In terms of these correlators equation (4.21) becomes

$$\begin{aligned}\frac{\mathrm{d}\rho_S}{\mathrm{d}t} = -\sum_{k=l,\epsilon_l=\epsilon_k}\int\frac{\mathrm{d}\omega}{2\pi}\int_0^\infty \mathrm{d}\tau\mathrm{e}^{-i\omega\tau}&\\ \Big[F_{kl}(\omega)\mathrm{e}^{-i\epsilon_l\tau}(S_k^\dagger S_l\rho_S(t) - S_l\rho_S(t)S_k^\dagger) + F_{kl}^*(-\omega)\mathrm{e}^{i\epsilon_l\tau}(\rho_S(t)S_l^\dagger S_k - S_k\rho_S(t)S_l^\dagger)&\\ +G_{kl}(\omega)\mathrm{e}^{i\epsilon_l\tau}(S_kS_l^\dagger\rho_S(t) - S_l^\dagger\rho_S(t)S_k) + G_{kl}^*(-\omega)\mathrm{e}^{-i\epsilon_l\tau}(\rho_S(t)S_lS_k^\dagger - S_k^\dagger\rho_S(t)S_l)\Big]&\end{aligned} \tag{4.23}$$

We now have integrals of type

$$\int\frac{\mathrm{d}\omega}{2\pi}F_{kl}(\omega)\int_0^\infty \mathrm{d}\tau\mathrm{e}^{-i(\omega+\epsilon_l)\tau} = \frac{1}{2}F_{kl}(-\epsilon_l) - iP\int\frac{\mathrm{d}\omega}{2\pi}\frac{F_{kl}(\omega)}{\omega+\epsilon_l} = \frac{\gamma_{Fkl} - i\xi_{Fkl}}{2}, \tag{4.24}$$

where P denotes the Cauchy principal value and is needed because the integral generally does not converge.[9] Now equation (4.23) becomes

$$\begin{aligned}\frac{\mathrm{d}\rho_S}{\mathrm{d}t} = \sum_{k=l,\epsilon_l=\epsilon_k} \Bigg[& \gamma_{Fkl}(S_l\rho_S(t)S_k^\dagger - \frac{1}{2}\{S_k^\dagger S_l, \rho_S(t)\}) + i\frac{\xi_{Fkl}}{2}[S_k^\dagger S_l, \rho_S(t)] \\ & + \gamma_{Gkl}(S_l^\dagger\rho_S(t)S_k - \frac{1}{2}\{S_k S_l^\dagger, \rho_S(t)\}) + i\frac{\xi_{Gkl}}{2}[S_k S_l^\dagger, \rho_S(t)]\Bigg],\end{aligned} \tag{4.25}$$

where $\gamma_{Gkl} = G_{kl}(\epsilon_l)$ and $\xi_{Gkl} = 2P\int \frac{\mathrm{d}\omega}{2\pi}\frac{G_{kl}(\omega)}{\omega-\epsilon_l}$.

Going back to the Schrödinger picture we get

$$\begin{aligned}\frac{\mathrm{d}\rho_S(t)}{\mathrm{d}t} = & -i[H_S + H_{LS}, \rho_S] \\ & + \sum_{k=l,\epsilon_l=\epsilon_k} \left[\gamma_{Fkl}(S_l\rho_S S_k^\dagger - \frac{1}{2}\{S_k^\dagger S_l, \rho_S\}) + \gamma_{Gkl}(S_l^\dagger\rho_S S_k - \frac{1}{2}\{S_k S_l^\dagger, \rho_S\})\right],\end{aligned} \tag{4.26}$$

where

$$H_{LS} = -\sum_{k=l,\epsilon_l=\epsilon_k}\left(\frac{\xi_{Fkl}}{2}S_k^\dagger S_l + \frac{\xi_{Gkl}}{2}S_k S_l^\dagger\right) \tag{4.27}$$

is the so-called Lamb shift Hamiltonian, describing a renormalization of the system Hamiltonian due to its interaction with the bath.

Equation (4.26) is the Lindblad equation. It is a quantum mechanical analogy to the classical master equation. To use this equation one needs to find the suitable system-reservoir interaction, or the Lindblad operators S_k, and the rates γ associated with the interaction.

4.2.3 Example: bosons coupled to an external boson field

A Hamiltonian for N degenerate bosons interacting with an external boson field is similar to the Jaynes-Cummings Hamiltonian

$$H = \Omega\sum_j a_j^\dagger a_j + \sum_n \omega_n b_n^\dagger b_n + \sum_n\sum_j g_{nj}(a_j^\dagger b_n + a_j b_n^\dagger), \tag{4.28}$$

where a_j is the annihilation operator for a boson in the observable system and b_n is an annihilation operator in the external field. The interaction term consists of annihilating a boson either in the system or in the external field, and simultaneously creating a boson in the other. We consider this Hamiltonian because in the case of a single boson $N = 1$ it describes the SPP state coupling to an external field, and if we replace a_j with $\sigma_{-,j}$, the Hamiltonian describes the coupling of the degenerate molecule excitation states with an external field.

In the notation of section 4.2.2

$$S_j = a_j, \quad S_j(t) = a_j e^{-i\Omega t} \tag{4.29}$$

and

$$R_j = \sum_n g_{nj} b_n, \quad R_j(t) = \sum_n g_{nj} b_n e^{-i\omega_n t}. \tag{4.30}$$

This leads to simple correlators in the external field

$$\begin{aligned} \langle b_n^\dagger b_m \rangle &= \mathrm{Tr}_R(b_n^\dagger b_m \rho_R) = \delta_{nm} N(\omega_n) \\ \langle b_n b_m^\dagger \rangle &= \mathrm{Tr}_R(b_n b_m^\dagger \rho_R) = \delta_{nm}(N(\omega_n)+1), \end{aligned} \tag{4.31}$$

where on the second line we used the bosonic commutation relation $[b_n, b_m^\dagger] = \delta_{nm}$. The function $N(\omega_n) = \mathrm{Tr}_R(b_n^\dagger b_n \rho_R)$ is the average of the number operator, i.e., the distribution function. If the bath is in equilibrium $N(\omega_n) = \frac{1}{e^{\beta\omega_n - 1}}$ is the Bose-Einstein distribution.

Following section 4.2.2 we get

$$\begin{aligned} F_{jk}(\omega) = F_{kj}^*(\omega) &= \int \mathrm{d}t_1 \mathrm{e}^{i\omega t_1} \mathrm{Tr}_R(R_j(0) R_k^\dagger(t_1) \rho_R) \\ &= \sum_n g_{nj} g_{nk} (N(\omega_n)+1) \int \mathrm{d}t_1 e^{i(\omega+\omega_n)t_1} \\ &= \sum_n g_{nj} g_{nk} (N(\omega_n)+1) 2\pi\delta(\omega+\omega_n) \end{aligned} \tag{4.32}$$

and similarly

$$\begin{aligned} G_{jk}(\omega) = G_{kj}^*(\omega) &= \int \mathrm{d}t_1 \mathrm{e}^{i\omega t_1} \mathrm{Tr}_R(R_j^\dagger(t_1) R_k(0) \rho_R) \\ &= \sum_n g_{nj} g_{nk} N(\omega_n) 2\pi\delta(\omega+\omega_n). \end{aligned} \tag{4.33}$$

Plugging these into equation (4.24) we get

$$\begin{aligned} \int \frac{\mathrm{d}\omega}{2\pi} F_{jk}(\omega) \int_0^\infty \mathrm{d}\tau e^{-i(\omega+\Omega)\tau} &= \sum_n g_{nj} g_{nk} (N(\omega_n)+1) \int_0^\infty \mathrm{d}\tau e^{-i(-\omega_n+\Omega)\tau} \\ &= \int \mathrm{d}\omega J_{jk}(\omega)(N(\omega)+1)(\pi\delta(\omega-\Omega) - P\frac{i}{\Omega-\omega}) \\ &= \underbrace{\pi g_j(\Omega) g_k(\Omega)(N(\Omega)+1)}_{\Gamma_{Fjk}/2} - i \underbrace{P\int \mathrm{d}\omega \frac{g_j(\omega) g_k(\omega)}{(\Omega-\omega)}(N(\omega)+1)}_{\xi_{Fjk}/2}, \end{aligned} \tag{4.34}$$

where we have assumed that the states n in the external field are so dense that we can replace the sum with an integral using the so-called spectral density $J_{jk}(\omega)$

$$\sum_n g_{nj} g_{nk} \to \int \mathrm{d}\omega J_{jk}(\omega). \tag{4.35}$$

A similar procedure for the other three terms in equation (4.23) leads to the Lindblad equation (in the Shrödinger picture)

$$\frac{\mathrm{d}\rho_S}{\mathrm{d}t} = -i[H_S, \rho_S] + \sum_{jk} \left[\Gamma_{Fjk}(a_k \rho_S a_j^\dagger - \frac{1}{2}\{a_j^\dagger a_k, \rho_S\}) + \Gamma_{Gjk}(a_k^\dagger \rho_S a_j - \frac{1}{2}\{a_j a_k^\dagger, \rho_S\}) \right], \tag{4.36}$$

where the Lamb-shift Hamiltonian containing the Cauchy principal value integral has been neglected since it only causes a small renormalization of the system Hamiltonian (see Appendix B). The decay and excitation rates are

$$\Gamma_{Fjk} = 2\pi J_{jk}(\Omega)(N(\Omega)+1) \quad \text{and} \quad \Gamma_{Gjk} = 2\pi J_{jk}(\Omega)N(\Omega), \tag{4.37}$$

respectively.

Equation (4.36) gives us general forms for the Lindblad terms for decay and excitation. The second term represents decay of the system excitation into the external field, while the last term represents the external field exciting the system.

5 Lindblad equation for the strong coupling system

In this section we construct a Lindblad equation for the SPP–molecule system. We consider different processes that may cause dissipation in the system. First we consider decay of the SPP excitation and molecule excitations into separate external electromagnetic fields. To get access to a stationary solution, we consider a process where an external field causes also excitations in the system.

In addition to the external electromagnetic field we add an external bath of phonons that scatter off the molecules. We assume that this interaction happens individually for each molecule i.e. the molecules are all coupled to separate baths. Elastic scattering causes dephasing, that partially destroys interference in the system. We also consider inelastic scattering, that causes dissipation of energy in the molecule states.

Our model for the Lindblad equation assumes that, even though there is a strong coupling between the SPP and molecules, the interaction with the environment happens separately, i.e., in the derivation of the Lindblad equation we neglect the strong coupling. This is not a very good approximation, but we hope that the essential physics stays undisturbed in this toy model.

5.1 Decay and excitation

First we consider decay and excitation in the form given by equation (4.36). We are interested in the polarization of the light emitted by the system into the external field. Because of that we explicitly write the polarization dependence of the coupling while all other effects are left implicit in the coupling constant. For example the coupling constant for the coupling of the SPP mode into the external field that has polarization into x-direction, can be written as $g_{px}(\omega) = g_p(\omega)(\hat{u}_p \cdot \hat{u}_x)$.

SPP decay

We assume that the external fields with different polarizations do not correlate, i.e. they produce separate decay terms in the Lindblad equation. We also assume that there is rotational symmetry between the external fields, i.e., the external field correlators between two operators with the same polarization are the same for all the polarizations. Since the SPP mode can only be p-polarized, it can only relax by emitting p-polarized light. These assumptions give us the SPP decay term

$$\mathcal{L}_{L_p}[\rho] = \Gamma_p \left[(\hat{u}_p \cdot \hat{u}_z)^2 (L_p \rho L_p^\dagger - \frac{1}{2}\{L_p^\dagger L_p, \rho\}) + (\hat{u}_p \cdot \hat{u}_x)^2 (L_p \rho L_p^\dagger - \frac{1}{2}\{L_p^\dagger L_p, \rho\}) \right], \quad (5.1)$$

where $\Gamma_p = \pi J_p(E_p)(N(E_p)+1)$ is the SPP decay rate and $L_p^\dagger = |p\rangle\langle 0|$ creates a SPP in the system. For energies in the optical range, $\sim 1\,\mathrm{eV}$, the Bose function at room temperature (or below) approaches zero, thus the SPP relaxation rate $\Gamma_p \to \pi J_p(E_p)$ and the direct excitation of SPPs can be neglected.

Molecule decay

A decay term for the molecules in the form of equation (4.36) is

$$\mathcal{L}_{L_j}[\rho] = \Gamma_m \sum_{jk=1}^{N} \sum_{\sigma=x,y,z} (\hat{n}_j \cdot \hat{u}_\sigma)(\hat{n}_k \cdot \hat{u}_\sigma)(L_j \rho L_k^\dagger - \frac{1}{2}\{L_k^\dagger L_j, \rho\}), \tag{5.2}$$

where $\Gamma_m = \pi J_m(E_m)$ is the molecule decay rate and $L_j^\dagger = |j\rangle\langle 0|$ excites the jth molecule. The Bose function has been neglected similarly to the SPP decay. It is useful to note that, because of the degeneracy of the molecule states, the decay term contains cross terms between different molecules. If the molecule states were non-degenerate, or if they coupled to separate external baths, there would be a Kronecker delta, δ_{jk}, that would not allow for the cross terms.

Excitation

We add pumping to the bonding hybrid state $|b\rangle$. The pumping can be included by adding an excitation term

$$\mathcal{L}_{L_b^\dagger}[\rho] = \Gamma_{exc}(L_b^\dagger \rho L_b - \frac{1}{2}\{L_b L_b^\dagger, \rho\}), \tag{5.3}$$

where $L_b^\dagger = |b\rangle\langle 0|$. Adding the excitation term allows the system to reach a stationary state other than the vacuum state.

5.2 Dephasing

Dephasing is a process where the external reservoir produces fluctuations in the system without changing populations of the states or changing the average energy. These fluctuations lead to a loss of interference between different states of the system. This is seen as decay of the off-diagonal terms of the density matrix.[15]

We consider a model where phonons in an external bath scatter elastically off the molecules. Elastic scattering does not change the average energy of the system.

The Hamiltonian describing dephasing caused by the external field affecting a single molecule is

$$H_{\phi,j} = \omega_m P_j + \sum_n \omega_n b_n^\dagger b_n + \sum_n g_{nj} P_j (b_n + b_n^\dagger), \tag{5.4}$$

where $P_j = |j\rangle\langle j| = L_j^\dagger L_j$ is a projection operator to the state $|j\rangle$ and thus satisfies $P_j^2 = P_j = P_j^\dagger$. Here we have chosen to treat dephasing locally so that it affects each molecule individually. The interaction term commutes with the system Hamiltonian $\omega_m P_j$, so it does not cause relaxation or excitation in the system. However, it does lead to a dephasing term in the Lindblad equation when we trace out the environment.

The dephasing Lindblad term is

$$\mathcal{L}_{P_j}[\rho] = \Gamma_\phi \sum_{j=1}^{N} (P_j \rho P_j - \frac{1}{2}\{P_j, \rho\}), \tag{5.5}$$

where the dephasing rate $\Gamma_\phi = 2\pi J_j(0)N(0)$. Since the Bose-Einstein distribution approaches infinity as the frequency goes to zero, we have to be careful with what we mean by $J_j(0)N(0)$. It is to be understood as the limit $\lim_{\omega\to 0} J_j(\omega)N(\omega)$. Now to get a finite dephasing rate, the spectral density, proportional to the coupling, $J_j(\omega)$ must go to zero sufficiently fast as frequency goes to zero.[14]

We neglect the Lamb shift term

$$i\sum_j \Delta_j[P_j,\rho] = i\sum_j P\int \mathrm{d}\omega \frac{g_j^2(\omega)}{\omega}(2N(\omega)+1)[P_j,\rho] \tag{5.6}$$

as we expect the energy shift Δ_j to be small compared to the other energies in the system.

5.3 Inelastic scattering with phonons

The same phonons that cause dephasing may also scatter inelastically, that inelastic scattering may cause the decay of an individual molecule excitation. The Lindblad term describing the inelastic scattering is

$$\mathcal{L}_{L_{\Delta j}}[\rho] = \Gamma_\Delta \sum_{j=1}^{N}\sum_{\sigma=x,y,z}(\hat{n}_j\cdot\hat{u}_\sigma)^2(L_j\rho L_j^\dagger - \frac{1}{2}\{L_j^\dagger L_j,\rho\}) \tag{5.7}$$

where Γ_Δ is the decay rate due to inelastic scattering. Since the decay of the molecule excitations due to inelastic scattering emits phonons it does not contribute to the emission of light.

The complete Lindblad equation with excitation into the hybrid states, SPP and molecule decay, dephasing and inelastic scattering is

$$\begin{aligned}\dot{\rho} =& i[\rho,H] + \Gamma_\phi\sum_{j=1}^{N}(P_j\rho P_j - \frac{1}{2}\{P_j,\rho\}) + \Gamma_{exc}(L_b^\dagger\rho L_b - \frac{1}{2}\{L_bL_b^\dagger,\rho\})\\ &+\Gamma_p\left[(\hat{u}_p\cdot\hat{u}_z)^2(L_p\rho L_p^\dagger - \frac{1}{2}\{L_p^\dagger L_p,\rho\}) + (\hat{u}_p\cdot\hat{u}_x)^2(L_p\rho L_p^\dagger - \frac{1}{2}\{L_p^\dagger L_p,\rho\})\right]\\ &+\Gamma_m\sum_{jk=1}^{N}\sum_{\sigma=x,y,z}(\hat{n}_j\cdot\hat{u}_\sigma)(\hat{n}_k\cdot\hat{u}_\sigma)(L_j\rho L_k^\dagger - \frac{1}{2}\{L_k^\dagger L_j,\rho\})\\ &+\Gamma_\Delta\sum_{j=1}^{N}\sum_{\sigma=x,y,z}(\hat{n}_j\cdot\hat{u}_\sigma)^2(L_j\rho L_j^\dagger - \frac{1}{2}\{L_j^\dagger L_j,\rho\}),\end{aligned} \tag{5.8}$$

where H is the strong coupling Hamiltonian (3.5). The rest of this thesis is dedicated to finding the solution to this Lindblad equation. In section 6 we limit the case to only few molecules and find the numerical solution to get an understanding of the behavior of the system. Using the observations from the numerical solution we then find an analytical solution under some simplifying assumptions in section 7.

6 Numerical solution with few molecules

Since the Lindblad equation is a $(N+2)\times(N+2)$-dimensional matrix differential equation it is advisable to try to find limits where some of the matrix elements can be neglected. In this section we discuss a numerical solution to the Lindblad equation (5.8) in a simple case of just two molecules, $N = 2$, to get a better understanding of what the relevant limits are. The two molecule case however is not big enough to show some of the properties of the solution, so to support it we also look at the $N = 4$ case.

We trust that the results obtained are general enough to justify the assumptions that are necessary for the analytical solution for a large number of molecules ($N \to \infty$) in the next section. The rigorous proof of the validity of these assumptions is left as an open question for further research.

In finding the analytical solution we make two assumptions:

- Because of the excitation term the system evolves into a stationary state, for which the density matrix is independent of time $\dot{\rho} = 0$.
- If the rates of the dissipative processes are small compared to the coupling inside the system, the off-diagonal terms of the density matrix in the eigenbasis vanish in the stationary state.

The validity of these assumptions is supported by the numerical solution. In section 6.3 we look at the properties of the stationary solution. The second assumption is discussed in terms of the numerical solution in section 6.2.

In addition to the two assumptions we make several observations about the numerical solution. These observations, while interesting, may not aid us in finding the analytical solution.

6.1 Numerical methods

We used the Wolfram Mathematica 10.4 [16] software to write the Lindblad equation in an orthonormal eigenbasis. The eigenbasis was determined by using the `Eigensystem` function, which for numerical matrices determines the eigenvalues and an eigenbasis of independent vectors.[17] The eigenvectors were checked to be orthonormal. That was done by first storing the eigenvectors in a matrix and checking that the conjugate transpose of the matrix times the matrix gives a unit matrix.

We then used the `DSolve` [18] function to solve the 4×4 (or 6×6 in the case of 4 molecules) system of differential equations. The full code can be found in Appendix C.

The accuracy of the numerical treatment is mainly limited by two error sources, the intrinsic accuracy of the numerical method and the precision of the numbers. We used decimal numbers, that are stored with machine precision. The functions `Eigensystem` and `DSolve` were able to give out results with the same machine precision. The machine precision in Mathematica corresponds to numbers that can be expressed with 53 binary bits.[19] Even this level of precision is much more than we actually need. In this section we are only interested in the behaviour of the density matrix in different limits and the

actual numbers are not that important.

The molecule dipole moments were given by

$$\hat{n}_j = \{\sin(\theta_j)\cos(\phi_j), \sin(\theta_j)\sin(\phi_j), \cos(\theta_j)\}, \tag{6.1}$$

where the angles $\theta_j = \frac{\pi(j-1)}{N-1}$ and $\phi_j = \frac{2\pi(j-1)}{N-1}$ were evenly distributed. The SPP polarization was into z-direction

$$\hat{u}_p = \{0, 0, 1\}. \tag{6.2}$$

The molecule state energy was set to $\omega_m = 10g$. Excitation of the system was only into the bonding hybrid state $|b\rangle$. For most of the calculations the system was initially prepared into the bonding state $|b\rangle$, i.e. $\rho_{bb}(0)$ was set to 1 and all other elements were 0. The coupling constant was set to $g = 1$, and the units in the numerics were set accordingly so that for example the time coordinate used is the time in SI-units divided by g, $t = t_{SI}/g$.

6.2 System-environment interaction rates

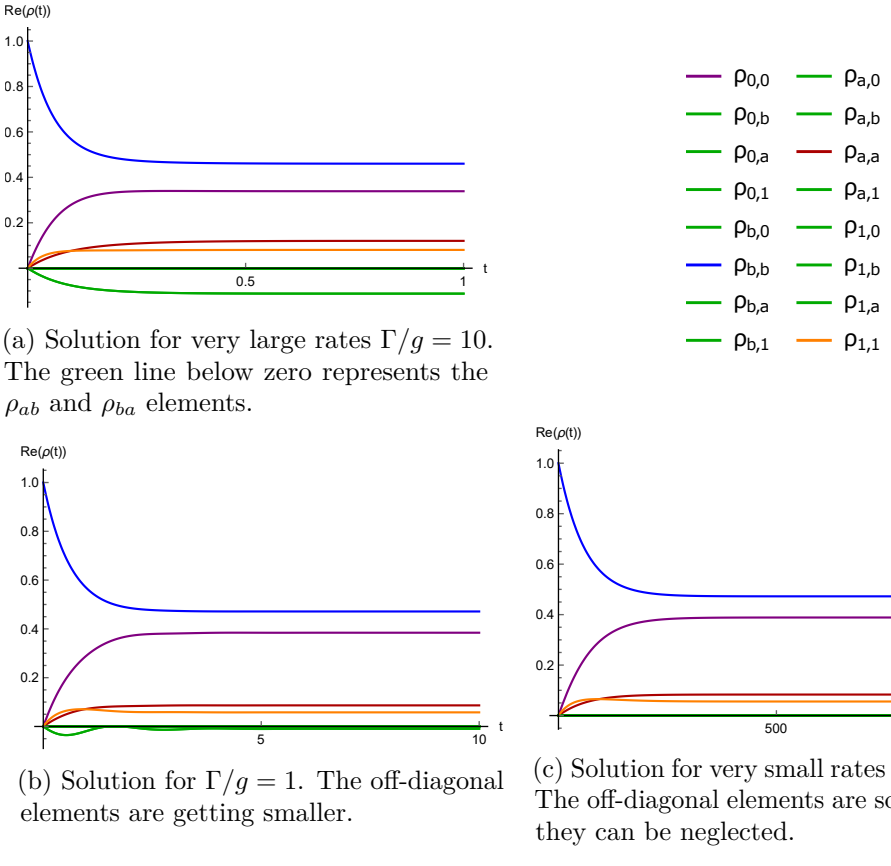

(a) Solution for very large rates $\Gamma/g = 10$. The green line below zero represents the ρ_{ab} and ρ_{ba} elements.

(b) Solution for $\Gamma/g = 1$. The off-diagonal elements are getting smaller.

(c) Solution for very small rates $\Gamma/g = 0.01$. The off-diagonal elements are so small that they can be neglected.

Figure 6.1: Real part of the density matrix, solved from the Lindblad equation without inelastic scattering $\Gamma_\Delta = 0$, with different process rates $\Gamma_{exc} = \Gamma_p = \Gamma_m = \Gamma_\phi = \Gamma$. Coupling constant is set to $g = 1$ and the system is near resonance $\delta = 0.01$. With very large process rates the solution has off-diagonal elements (green line below zero) that do not vanish in the stationary limit. For very small process rates the off-diagonal elements essentially vanish.

There are several remarks to be made from the numerical solution in different limits. We begin by looking at how changing the rates Γ_i of the Lindblad processes affects the time evolution of the off-diagonal terms of the density matrix.

Figure 6.1 shows the real part of a numerical solution to the Lindblad equation with dephasing but without the inelastic scattering, i.e. $\Gamma_\Delta = 0$. The coupling constant is set to $g = 1$ and the system is near resonance with $\delta = 0.01$. Note that initially, at time $t = 0$, the density matrix has only one non-zero element $\rho_{bb} = 1$.

For large Γ_i the density matrix evolves in a way that creates off-diagonal terms. However the only off-diagonal elements that are created are ρ_{ab} and ρ_{ba}. When Γ_i are much smaller than the coupling (here $\Gamma_i/g = 0.01$) the off-diagonal terms get so small that they can be neglected.

The limit $\Gamma_i \ll g$ means that the interactions between the system and its surroundings are much weaker than the strong coupling inside the system. This a reasonable assumption in many open quantum systems and especially in our strong coupling system. The result that the off-diagonal terms vanish in this limit is made use of below in finding the analytical solution.

Four molecule case

The $N = 2$ case has only one molecule superposition state $|m\rangle$ and thus the density matrix does not have off-diagonal elements between molecule eigenstates. In the $N = 4$ case, however, there are three molecule superposition states and the density matrix can have off-diagonal elements between the molecule eigenstates. We still need to find out how they evolve.

Using the same parameters as above the Lindblad equation can be solved for the $N = 4$ case. The time evolution of the real part of the density matrix is shown in figure 6.2. It can be easily noticed that there are now off-diagonal elements even after long time has passed and even with small interaction rates. The off-diagonal elements that remain are elements between the molecule superposition states. The off-diagonal elements involving hybrid states still disappear with reducing interaction rates.

The molecule superposition states are degenerate eigenstates of the strong coupling Hamiltonian (3.5) with energy $\delta/2$. As discussed in section 3.3 there is some freedom in choosing the degenerate eigenstates. Because of this freedom there is probably an eigenbasis where the off-diagonal molecule state-molecule state elements vanish.

It is evident that the basis that was obtained with the `Eigensystem` function in Mathematica was not the best choice for the eigenbasis. The proper choice for the molecule superposition states is an open question in the scope of this thesis. In this section we proceed with the two-molecule case where this problem does not exist. For the analytical solution in section 7 we use the spherical harmonics basis specified in section 3.3. We trust that the results that we obtain still have some merit even if the molecule superposition states may not be chosen properly.

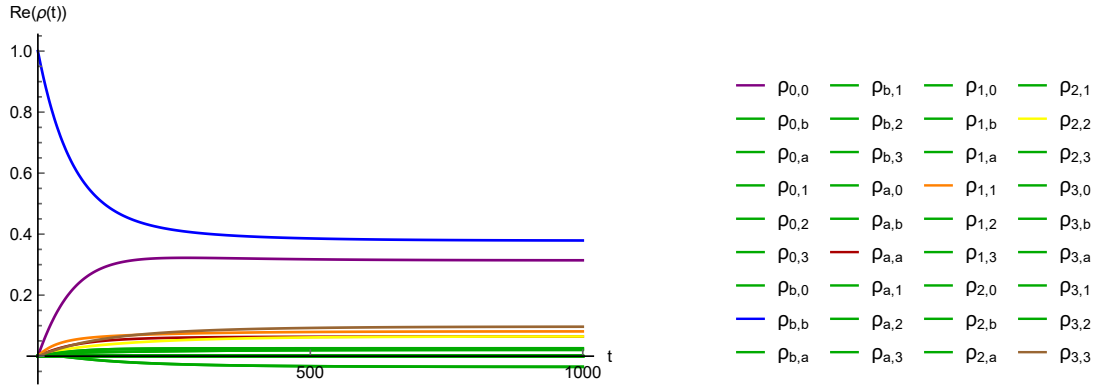

(a) Solution for small rates $\Gamma/g = 0.01$.

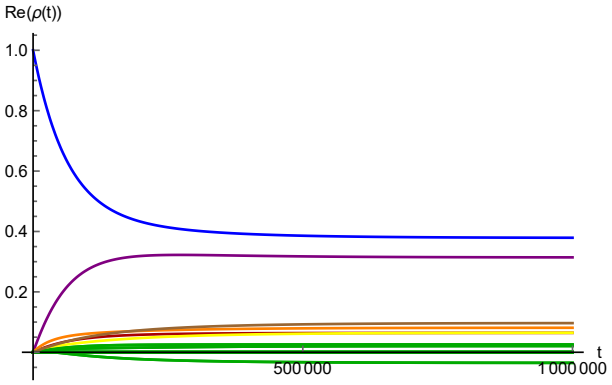

(b) Solution for very small rates $\Gamma/g = 10^{-4}$.

Figure 6.2: $N = 4$. Real part of the density matrix, solved from the Lindblad equation with dephasing, $\Gamma_{exc} = \Gamma_p = \Gamma_p = \Gamma_\phi = \Gamma$, $\Gamma_\Delta = 0$. Coupling constant is set to $g = 1$ and the system is near resonance $\delta = 0.01$. The off-diagonal molecule-molecule elements do not vanish with a smaller Γ/g ratio.

6.3 Stationary solution and the energy difference

Proceeding with the $N = 2$ case we look at what effect the excitation term has and how the system evolves into the stationary solution. We also look at what happens when the SPP and molecules are far from resonance, quantified by the energy difference $\delta = \omega_m - \omega_p$.

Stationary solution

Due to the excitation the density matrix reaches a stationary state where the matrix elements no longer change with time. The time it takes for the system to reach the stationary state, the relaxation time τ, depends on the strength of the system-environment coupling. In figure 6.1 the relaxation time is proportional to $1/\Gamma$. Without the excitation term the system always eventually decays into the vacuum state, see figure 6.3.

Changing the initial state of the system from $|b\rangle$ to any other state does not change the stationary state. For example in figure 6.1c the initial state is $|b\rangle$, changing the initial state to $|\psi\rangle = \frac{1}{\sqrt{2}}(|a\rangle + |b\rangle)$ (or $\rho(0) = |\psi\rangle\langle\psi|$ in terms of the density matrix) changes the diagonal elements of the solution in the long-time limit ($t \to \infty$) by $\sim \pm 1/t$. In other words in the long time limit the solutions with different initial states approach each other.

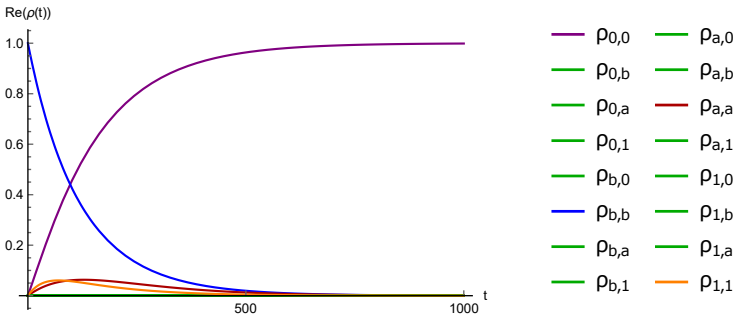

Figure 6.3: Real part of the density matrix without excitation and inelastic scattering, i.e. $\Gamma_{exc} = \Gamma_\Delta = 0$, $\Gamma_p = \Gamma_m = \Gamma_\phi = \Gamma$. Without excitation the system eventually decays into the vacuum state.

Thus the stationary state does not depend on the initial state. Figure 6.4 shows the solutions with different initial states.

The existence of a stationary state makes the system easier to solve in the case of many molecules. Instead of solving the full matrix differential equation we can let the system evolve into the stationary state. In the stationary state we can set $\dot{\rho} = 0$ and we are left with just a linear system of equations.

Near and far from resonance

The difference between the energies of the molecule states and the SPP state, $\delta = \omega_m - \omega_p$, represents how far from resonance the system is. Figure 6.5 shows the solution to the Lindblad equation with dephasing with different values of δ.

Increasing δ leads to decreasing the population of the antibonding state and the molecule state. This is because with large positive values of δ the bonding state behaves like the free SPP state, see figure 3.1. For large negative values of δ the population of the antibonding state disappears, but the molecule state is much higher in population. This happens because the bonding state behaves like the free molecule state with large negative δ.

The difference between the populations of the bonding state and vacuum decreases as δ increases. Far from resonance when δ is positive the energy of the bonding state and the vacuum state are close in energy (see Figure 3.1). In the negative side, however, the bonding state energy is much higher than the vacuum energy and decay into vacuum is less likely.

At resonance the bonding state is much higher in population than the antibonding state. That is because there is excitation only into the bonding state.

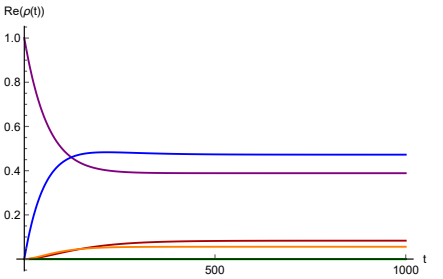

(a) Initial state $|0\rangle$.

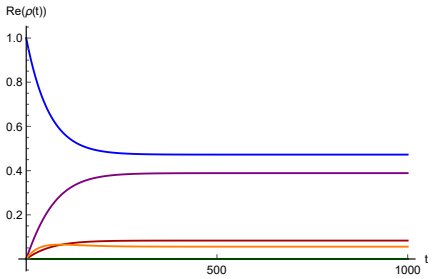

(b) Initial state $|b\rangle$.

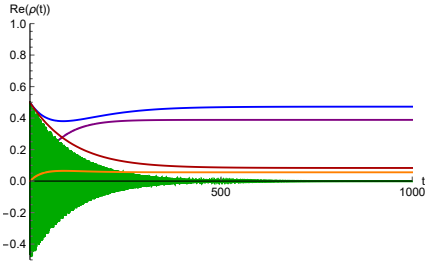

(c) Initial state $|\psi\rangle = \frac{1}{2}(|a\rangle + |b\rangle)$. The decaying off-diagonal terms are ρ_{ab} and ρ_{ba}.

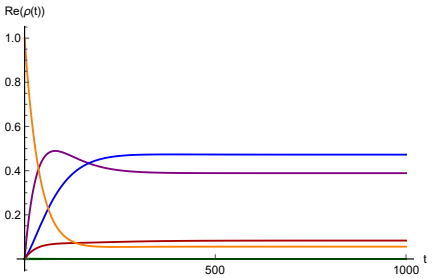

(d) Initial state $|m = 1\rangle$.

Figure 6.4: Evolution of different initial states. Other parameters are as in figure 6.1c. The initial state does not significantly change the stationary state.

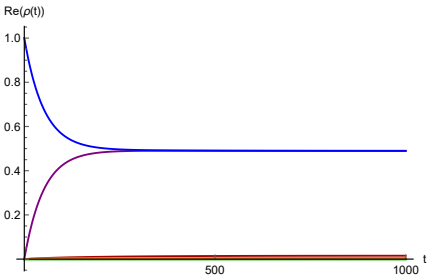

(a) Solution with large positive $\delta = 9$.

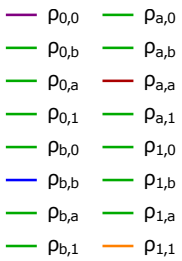

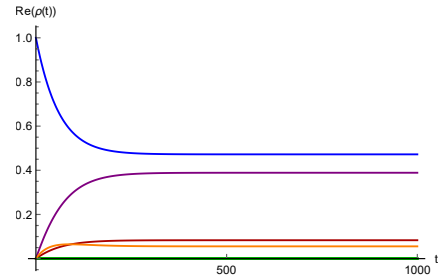

(b) Solution at resonance $\delta = 0$.

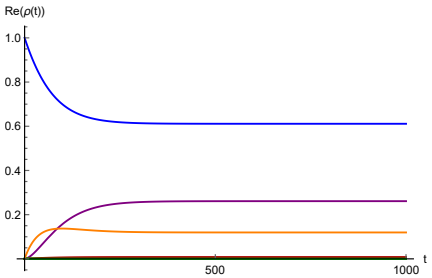

(c) Solution with large negative $\delta = -9$.

Figure 6.5: Real part of the density matrix, solved from the Lindblad equation with dephasing, $\Gamma_{exc} = \Gamma_p = \Gamma_p = \Gamma_\phi = \Gamma, \Gamma_\Delta = 0$. Far from resonance the system starts to behave more like the free SPP state (for positive δ) or the free molecule state (for negative δ).

6.4 Effect of dephasing and inelastic scattering

Dephasing

Above the Lindblad equation we numerically solve always has the dephasing term. Figure 6.6 shows the real part of the solution to the Lindblad equation without dephasing and without inelastic scattering using otherwise the same parameters as figure 6.1c. Without dephasing the only non-zero matrix elements in the stationary solution are ρ_{00} and ρ_{bb}. Thus it is due to the dephasing term that the stationary solution in, for example, figure 6.4, has non-zero elements on the whole diagonal. The stationary solution with dephasing is a statistical mixture of all of the eigenstates, while without dephasing only the vacuum state $|0\rangle$ and bonding state $|b\rangle$ are allowed.

The excitation of the hybrid molecule states takes energy, but the dephasing term is not supposed to change the total energy of the system. The addition of the dephasing term seems to violate energy conservation. This is because of the way we construct the Lindblad equation in section 5, where we neglect the strong coupling. At the expense of momentum conservation energy could be conserved, if we let the SPP transfer to a different momentum.

If the initial state has off-diagonal elements, e.g. $\rho(0) = |\psi\rangle\langle\psi| = \frac{1}{2}(|b\rangle\langle b| + |a\rangle\langle a| + |a\rangle\langle b| + |b\rangle\langle a|)$, the off-diagonal elements decay with and without dephasing. However dephasing causes the off-diagonal elements to decay faster. Without dephasing in figure 6.6b the off-diagonal elements decay with the same rate as the antibonding element ρ_{aa}. With dephasing in figure 6.4c the decay of the off-diagonal elements is faster.

In conclusion, the dephasing term allows the stationary state to be a statistical mixture of all of the eigenstates and makes the decay of the off-diagonal terms faster.

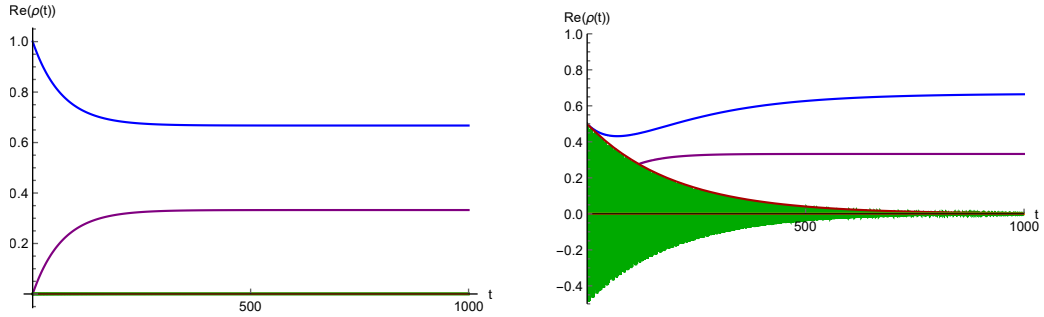

(a) Initial state $|b\rangle$.

(b) Initial state $|\psi\rangle = \frac{1}{\sqrt{2}}(|a\rangle + |b\rangle)$.

Figure 6.6: Real part of the solution without dephasing $\Gamma_\phi = 0$ and without the inelastic scattering $\Gamma_\Delta = 0$. Parameters are otherwise as in figure 6.1c. Without dephasing the stationary solution does not have the antibonding or the molecule superposition states. When the initial state contains off-diagonal elements, figure 6.6b, they decay with the same rate as the antibonding state (red line) decays.

Inelastic scattering

In the numerical solution inelastic scattering term, proportional to the inelastic decay rate Γ_Δ, only changes the populations of the states in the stationary state. The change in

population is proportional to Γ_Δ, the bigger the ratio between the inelastic decay rate and the other interaction rates, the bigger an effect inelastic scattering has on the populations. Figure 6.7 shows the real part of the solution with inelastic scattering. Inelastic scattering does not contribute to the emission of photons from the system and to simplify the analytical solution we neglect this term.

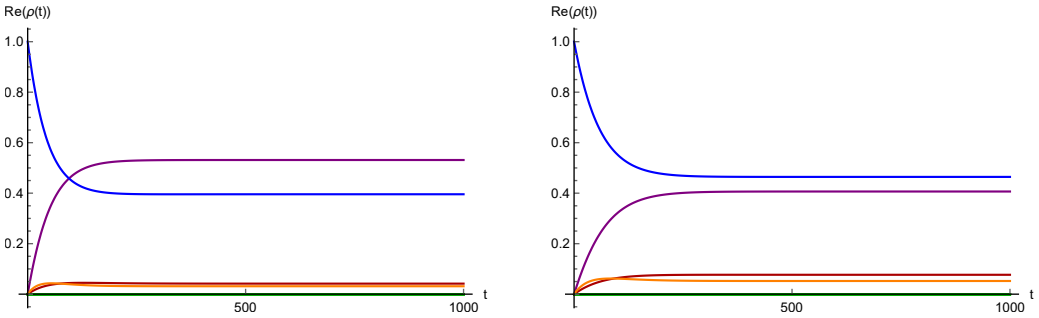

(a) Large inelastic decay rate $\Gamma_\Delta = 0.01 = \Gamma$.

(b) Small inelastic decay rate $\Gamma_\Delta = 0.001 = 0.1\Gamma$.

Figure 6.7: Real part of the solution with inelastic scattering. Parameters are otherwise as in figure 6.1c. Inelastic scattering raises the population of the vacuum state with the expense of the other states. The change in population is proportional to Γ_Δ.

7 Analytical solution

Equipped with the observations from the numerical solution we are now able to solve the Lindblad equation (5.8) analytically in the stationary state. We begin with the Lindblad equation (5.8) without inelastic scattering. Then we add a correction term and observe that it allows s-polarization in the light emitted from the system to the external field.

7.1 Dephasing Lindblad equation

We transform the Lindblad equation into the energy eigenbasis using the transformation specified in section 3.4. In the eigenbasis the density matrix can be written as

$$\rho = \sum_{h,h'} \rho_{hh'} |h\rangle\langle h'|, \tag{7.1}$$

where the h sums go over all eigenstates $h, h' = 0, a, b, m$. The unitary term does not have diagonal elements in the eigenbasis

$$i[\rho, H] = \sum_{h,k} \rho_{hk}(E_k - E_h)|h\rangle\langle k|, \tag{7.2}$$

where the h and k sums go over all eigenstates $h, k = 0, a, b, m$. The other terms in the Lindblad equation become

$$\begin{aligned}
L_b^\dagger \rho L_b - \frac{1}{2}\{L_b L_b^\dagger, \rho\} =& \rho_{00}|b\rangle\langle b| - \frac{1}{2}\sum_h (\rho_{0h}|0\rangle\langle h| + \rho_{h0}|h\rangle\langle 0|), \\
L_p \rho L_p^\dagger - \frac{1}{2}\{L_p^\dagger L_p, \rho\} =& \sum_{l,l'=a,b} \gamma_l^* \gamma_{l'} \rho_{ll'} |0\rangle\langle 0| \\
& - \frac{1}{2}\sum_{l,l'=a,b}\sum_h (\gamma_l \gamma_{l'}^* \rho_{l'h}|l\rangle\langle h| + \gamma_l \gamma_{l'}^* \rho_{hl}|h\rangle\langle l'|), \\
L_j \rho L_k^\dagger - \frac{1}{2}\{L_k^\dagger L_j, \rho\} =& \sum_{h,h'} \epsilon_{jh}^* \epsilon_{kh'} \rho_{hh'} |0\rangle\langle 0| \\
& - \frac{1}{2}\sum_{h_1,h_2,h_3} (\epsilon_{jh_3}^* \epsilon_{kh_2} \rho_{h_3h_1} + \epsilon_{jh_1}^* \epsilon_{kh_3} \rho_{h_2h_3})|h_2\rangle\langle h_1| \quad \text{and} \\
P_j \rho P_j - \frac{1}{2}\{P_j, \rho\} =& \sum_{h_1h_2h_3h_4} \epsilon_{jh_1} \epsilon_{jh_2}^* \epsilon_{jh_3} \epsilon_{jh_4}^* \rho_{h_2h_3} |h_1\rangle\langle h_4| \\
& - \frac{1}{2}\sum_{h_1h_2h_3} (\epsilon_{jh_1} \epsilon_{jh_2}^* \rho_{h_2h_3} + \epsilon_{jh_2} \epsilon_{jh_3}^* \rho_{h_1h_2})|h_1\rangle\langle h_3|,
\end{aligned} \tag{7.3}$$

where the h sums go over all the eigenstates and the l sums sum only the bonding and antibonding states.

Using the numerical results in section 6.2 as a guideline, we use the two assumptions of section 6. We assume that the system has had time to evolve into the stationary state $\rho_e = \lim_{t\to\infty}\rho(t)$, so that $\dot{\rho_e} = 0$. We also assume that the rates of the dissipative processes are small compared to the strong coupling inside the system, i.e. $\Gamma_i/g \to 0$ and that in this limit the off-diagonal elements of the density matrix vanish in the stationary state. With these assumptions the Lindblad equation reduces from an $(N+2)\times(N+2)$ system of differential equations into a system of $(N+2)$ ordinary equations.

The remaining $(N+2)$ equations in the eigenbasis are ($\Gamma_\Delta = 0$)

$$
\begin{aligned}
0 = \dot{\rho}_{00} =& \left(\Gamma_p u_p \frac{\omega_g-\delta}{2\omega_g} + \Gamma_m \frac{\omega_g+\delta}{2\omega_g}\frac{1}{\sum_l g_l^2}\sum_{jk=1}^{N} n_{jk} g_j g_k\right)\rho_{aa} \\
&+ \left(\Gamma_p u_p \frac{\omega_g+\delta}{2\omega_g} + \Gamma_m \frac{\omega_g-\delta}{2\omega_g}\frac{1}{\sum_l g_l^2}\sum_{jk=1}^{N} n_{jk} g_j g_k\right)\rho_{bb} \\
&+ \Gamma_m \sum_{jk=1}^{N} n_{jk}\sum_m \eta^*_{mk}\eta_{mj}\rho_{mm} - \Gamma_{exc}\rho_{00} \\
0 = \dot{\rho}_{aa} =& \left[\Gamma_\phi\left(\left(\frac{\omega_g+\delta}{2\omega_g}\right)^2 \frac{\sum_j g_j^4}{(\sum_l g_l^2)^2} - \frac{\omega_g+\delta}{2\omega_g}\right) - \Gamma_p u_p \frac{\omega_g-\delta}{2\omega_g} - \Gamma_m \frac{\omega_g+\delta}{2\omega_g}\frac{1}{\sum_l g_l^2}\sum_{jk=1}^{N} n_{jk} g_j g_k\right]\rho_{aa} \\
&+ \Gamma_\phi \frac{\sum_j g_j^4}{\omega_g^2 \sum_l g_l^2}\rho_{bb} + \Gamma_\phi \frac{\omega_g+\delta}{2\omega_g}\frac{1}{\sum_l g_l^2}\sum_j g_j^2 \sum_m \eta^*_{mj}\eta_{mj}\rho_{mm} \\
0 = \dot{\rho}_{bb} =& \left[\Gamma_\phi\left(\left(\frac{\omega_g-\delta}{2\omega_g}\right)^2 \frac{\sum_j g_j^4}{(\sum_l g_l^2)^2} - \frac{\omega_g-\delta}{2\omega_g}\right) - \Gamma_p u_p \frac{\omega_g+\delta}{2\omega_g} - \Gamma_m \frac{\omega_g-\delta}{2\omega_g}\frac{1}{\sum_l g_l^2}\sum_{jk=1}^{N} n_{jk} g_j g_k\right]\rho_{bb} \\
&+ \Gamma_\phi \frac{\sum_j g_j^4}{\omega_g^2 \sum_l g_l^2}\rho_{aa} + \Gamma_\phi \frac{\omega_g-\delta}{2\omega_g}\frac{1}{\sum_l g_l^2}\sum_j g_j^2 \sum_m \eta^*_{mj}\eta_{mj}\rho_{mm} + \Gamma_{exc}\rho_{00} \\
0 = \dot{\rho}_{nn} =& \Gamma_\phi \frac{\omega_g+\delta}{2\omega_g}\frac{1}{\sum_l g_l^2}\sum_{j=1}^{N} g_j^2 \eta^*_{nj}\eta_{nj}\rho_{aa} + \Gamma_\phi \frac{\omega_g-\delta}{2\omega_g}\frac{1}{\sum_l g_l^2}\sum_{j=1}^{N} g_j^2 \eta^*_{nj}\eta_{nj}\rho_{bb} \\
&- (\Gamma_m \sum_{jk=1}^{N} n_{jk}\eta^*_{nj}\eta_{nk} + \Gamma_\phi)\rho_{nn} + \Gamma_\phi \sum_{j=1}^{N}\eta^*_{nj}\eta_{nj}\sum_m \eta^*_{mj}\eta_{mj}\rho_{mm}.
\end{aligned}
\tag{7.4}
$$

Here $u_p = (\hat{u}_p\cdot\hat{u}_z)^2 + (\hat{u}_p\cdot\hat{u}_x)^2 = 1$, $n_{jk} = \sum_{\sigma=x,y,z}(\hat{n}_j\cdot\hat{u}_\sigma)(\hat{n}_k\cdot\hat{u}_\sigma)$ and we have substituted the basis transformation coefficients from section 3.4.

We assume in section 3.3 that the transition dipole moments of the molecules are evenly distributed in all directions. Now if the number of molecules is large, $N\to\infty$, we can replace the sums over all molecules by integrals as we did in section 3.3

$$
\sum_j \to \frac{N}{4\pi}\int_0^{2\pi} \mathrm{d}\phi_j \int_0^{\pi} \mathrm{d}\theta_j \sin(\theta_j). \tag{7.5}
$$

Writing the coupling constants in terms of the angles θ and ϕ as $g_j = g(\hat{n}_j\cdot\hat{u}_p) = g\cos\theta_j$ and the directions of the molecule dipole moments as $\hat{n}_j = (\sin\theta_j\cos\phi_j, \sin\theta_j\sin\phi_j, \cos\theta_j)$

allows us to evaluate some of the sums in equation (7.4):

$$\begin{aligned}
\sum_j g_j^2 =& \frac{Ng^2}{4\pi}\int_0^{2\pi} \mathrm{d}\phi \int_0^{\pi} \mathrm{d}\theta \sin\theta \cos^2\theta = \frac{Ng^2}{3} \\
\sum_j g_j^4 =& \frac{Ng^4}{4\pi}\int_0^{2\pi} \mathrm{d}\phi \int_0^{\pi} \mathrm{d}\theta \sin\theta \cos^4\theta = \frac{Ng^4}{5} \\
\sum_{jk} n_{jk} g_j g_k =& \frac{N^2 g^2}{16\pi^2}((\int_0^{2\pi} \mathrm{d}\phi \int_0^{\pi} \mathrm{d}\theta \sin\theta\cos\theta\sin\theta\cos\phi)^2 \\
&+ (\int_0^{2\pi} \mathrm{d}\phi \int_0^{\pi} \mathrm{d}\theta \sin\theta\cos\theta\sin\theta\sin\phi)^2 \\
&+ (\int_0^{2\pi} \mathrm{d}\phi \int_0^{\pi} \mathrm{d}\theta \sin\theta\cos\theta\cos\theta)^2) \\
=& \frac{N^2 g^2}{9}.
\end{aligned} \tag{7.6}$$

It is useful to note that here we chose the coordinate system where z'-direction is the SPP polarization direction and y'-direction is parallel to the surface. This coordinate system can be obtained from the natural coordinates that we use in section 2 by a rotation in the xz-plane.

We proceed by choosing the molecule superposition states with spherical harmonics coefficients (see section 3.3)

$$\eta_{mj} = \frac{1}{\sqrt{N}} Y_m^0(\theta_j, \phi_j) = \frac{1}{\sqrt{N}} \sqrt{2m+1} P_m(\cos\theta_j), \tag{7.7}$$

where $m = 0, 2, 3, \ldots, N$. Using the properties of the Legendre polynomials we can calculate almost all of the remaining sums over j:

$$\begin{aligned}
\sum_j g_j^2 \eta_{mj}^* \eta_{mj} =& \frac{Ng^2}{4\pi}\int_0^{2\pi} \mathrm{d}\phi \int_0^{\pi} \mathrm{d}\theta \sin\theta\cos^2\theta \frac{1}{N}(2m+1)P_m(\cos\theta)^2 \\
=& \frac{2m^2+2m-1}{(2m+3)(2m-1)} g^2 = A_m g^2 \\
\sum_{jk} n_{jk} \eta_{mk}^* \eta_{mj} =& \frac{N^2}{16\pi^2}((\int_0^{2\pi} \mathrm{d}\phi \int_0^{\pi} \mathrm{d}\theta \sin\theta\sin\theta\sin\phi \frac{1}{\sqrt{N}}\sqrt{2m+1}P_m(\cos\theta))^2 \\
&+ (\int_0^{2\pi} \mathrm{d}\phi \int_0^{\pi} \mathrm{d}\theta \sin\theta\sin\theta\cos\phi \frac{1}{\sqrt{N}}\sqrt{2m+1}P_m(\cos\theta))^2 \\
&+ (\int_0^{2\pi} \mathrm{d}\phi \int_0^{\pi} \mathrm{d}\theta \sin\theta\cos\theta \frac{1}{\sqrt{N}}\sqrt{2m+1}P_m(\cos\theta))^2 \\
=& 0
\end{aligned} \tag{7.8}$$

Substituting all the calculated sums into equation (7.4) we get

$$\begin{aligned}
0 = \dot{\rho}_{00} =& \left(\Gamma_p u_p \frac{\omega_g - \delta}{2\omega_g} + \Gamma_m \frac{N}{3}\frac{\omega_g + \delta}{2\omega_g}\right)\rho_{aa} + \left(\Gamma_p u_p \frac{\omega_g + \delta}{2\omega_g} + \Gamma_m \frac{N}{3}\frac{\omega_g - \delta}{2\omega_g}\right)\rho_{bb} \\
& - \Gamma_{exc}\rho_{00} \\
0 = \dot{\rho}_{aa} =& \left[\Gamma_\phi\left(\frac{9}{5N}\left(\frac{\omega_g + \delta}{2\omega_g}\right)^2 - \frac{\omega_g + \delta}{2\omega_g}\right) - \Gamma_p u_p \frac{\omega_g - \delta}{2\omega_g} - \Gamma_m \frac{N}{3}\frac{\omega_g + \delta}{2\omega_g}\right]\rho_{aa} \\
& + \Gamma_\phi \frac{9}{5N}\frac{(\omega_g + \delta)(\omega_g - \delta)}{(2\omega_g)^2}\rho_{bb} + \Gamma_\phi \frac{3}{N}\frac{\omega_g + \delta}{2\omega_g}\sum_m A_m \rho_{mm} \\
0 = \dot{\rho}_{bb} =& \left[\Gamma_\phi\left(\frac{9}{5N}\left(\frac{\omega_g - \delta}{2\omega_g}\right)^2 - \frac{\omega_g - \delta}{2\omega_g}\right) - \Gamma_p u_p \frac{\omega_g + \delta}{2\omega_g} - \Gamma_m \frac{N}{3}\frac{\omega_g - \delta}{2\omega_g}\right]\rho_{bb} \\
& + \Gamma_\phi \frac{9}{5N}\frac{(\omega_g + \delta)(\omega_g - \delta)}{(2\omega_g)^2}\rho_{aa} + \Gamma_\phi \frac{3}{N}\frac{\omega_g - \delta}{2\omega_g}\sum_m A_m \rho_{mm} + \Gamma_{exc}\rho_{00} \\
0 = \dot{\rho}_{nn} =& \Gamma_\phi \frac{3}{N}\frac{\omega_g + \delta}{2\omega_g} A_n \rho_{aa} + \Gamma_\phi \frac{3}{N}\frac{\omega_g - \delta}{2\omega_g} A_n \rho_{bb} \\
& - \Gamma_\phi \rho_{nn} + \Gamma_\phi \sum_{j=1}^{N} \eta_{nj}^* \eta_{nj} \sum_m \eta_{mj}^* \eta_{mj} \rho_{mm}.
\end{aligned} \tag{7.9}$$

Taking a sum over all the molecule states n of the last equation in (7.9) allows us to eliminate the sum $\sum_n A_n \rho_{nn}$ from the rest of the equations. Using the orthonormality condition (3.11) and the integrals calculated above we get

$$\Gamma_\phi \frac{3}{N}\sum_m A_m \rho_{mm} = \Gamma_\phi \frac{3}{N}\left(\frac{\omega_g + \delta}{2\omega_g}\rho_{aa} + \frac{\omega_g - \delta}{2\omega_g}\rho_{bb}\right)\sum_m A_m. \tag{7.10}$$

Equation (7.10) suggests that ρ_{mm} can be chosen so that they do not depend on m, so that

$$\rho_{mm} = \frac{\omega_g + \delta}{2\omega_g}\rho_{aa} + \frac{\omega_g - \delta}{2\omega_g}\rho_{bb} \tag{7.11}$$

for all $m \in \{0, 2, 3, \ldots, N-1\}$. We can calculate a value for $\sum_m A_m$ by taking a sum over m of the first equation in (7.8). Using the useful equation (3.22) we get

$$\sum_m A_m = \frac{N}{3} - \frac{3}{5} \tag{7.12}$$

Equation (7.10) can be replaced into the first three equations in (7.9) to obtain

$$\begin{aligned}
\rho_{00} =& \frac{1}{\Gamma_{exc}}\left(-\Gamma_p u_p \frac{\delta}{\omega_g} + \Gamma_m \frac{N}{3}\frac{\delta}{\omega_g} - \frac{\Gamma_p^2 u_p^2}{\Gamma_\phi} - \frac{\Gamma_p u_p \Gamma_m}{\Gamma_\phi}\frac{N}{3}\frac{2(\omega_g^2 + \delta^2)}{\omega_g^2 - \delta^2} + \frac{\Gamma_m^2}{\Gamma_\phi}\frac{N^2}{9}\right)\rho_{aa} \\
\rho_{bb} =& \left(1 + \frac{\Gamma_p u_p}{\Gamma_\phi}\frac{2\omega_g}{\omega_g + \delta} + \frac{\Gamma_m}{\Gamma_\phi}\frac{N}{3}\frac{2\omega_g}{\omega_g - \delta}\right)\rho_{aa}.
\end{aligned} \tag{7.13}$$

These can be substituted into equation (7.11) to get

$$\rho_{mm} = \left(1 + \frac{\Gamma_p u_p}{\Gamma_\phi}\frac{\omega_g - \delta}{\omega_g + \delta} + \frac{\Gamma_m}{\Gamma_\phi}\frac{N}{3}\right)\rho_{aa}, \tag{7.14}$$

for all $m \in \{0, 2, 3, \ldots, N-1\}$. Finally ρ_{aa} can be solved from the trace condition of the density matrix $\mathrm{Tr}(\rho) = \rho_{00} + \rho_{aa} + \rho_{bb} + \sum_n \rho_{nn} = 1$.

7.1.1 Origin of the emitted light

The $\dot{\rho}_{00}$ element of the Lindblad equation represents how the population of the vacuum state changes. All positive terms in the 00 element increase the population of the vacuum state, i.e. they describe decay into the vacuum. Negative terms describe excitation from the vacuum state and decrease the population. Since the decay into the vacuum state happens by emitting photons we can theoretically predict which part of the emitted photons is produced by different decay mechanisms.

Adding up the terms that come from SPP decay in the first equation in (7.9) we get the rate at which the stationary system emits light that comes from plasmon decay

$$f_p = \Gamma_p\left(\frac{\omega_g - \delta}{2\omega_g}\rho_{aa} + \frac{\omega_g + \delta}{2\omega_g}\rho_{bb}\right). \tag{7.15}$$

Similarly we can look at the molecule decay terms and get the rate at which the system emits light that came from molecule decay

$$f_m = \Gamma_m\frac{N}{3}\left(\frac{\omega_g + \delta}{2\omega_g}\rho_{aa} + \frac{\omega_g - \delta}{2\omega_g}\rho_{bb}\right). \tag{7.16}$$

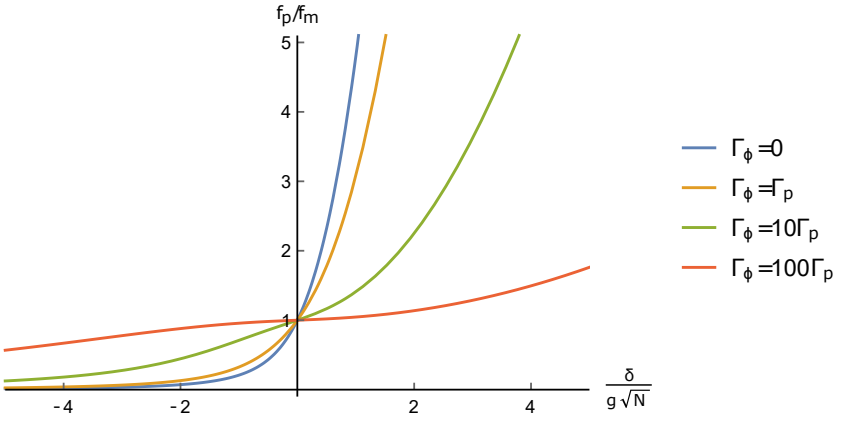

Figure 7.1: The ratio between the rate at which SPP decay emits light and the molecule decay emits light as a function of $\delta/\sqrt{N}g$, with different dephasing rates. The SPP decay rate is $\Gamma_p = \frac{N}{3}\Gamma_m$, so that at resonance the two rates are equal. Excitation is here into the bonding state $|b\rangle$. For an excitation into the antibonding state $|a\rangle$, the curve is the same but $\delta \to -\delta$.

Plugging in ρ_{bb} from equation (7.13), the ratio between the rate at which the SPP decay emits light and the rate at which the molecule decay emits light becomes

$$\frac{f_p}{f_m} = \frac{\Gamma_p(\Gamma_p(\omega_g - \delta)(\omega_g + \delta) + \frac{N}{3}\Gamma_m(\omega_g + \delta)^2 + \Gamma_\phi(\omega_g - \delta)(\omega_g + \delta))}{\frac{N}{3}\Gamma_m(\Gamma_p(\omega_g - \delta)^2 + \frac{N}{3}\Gamma_m(\omega_g - \delta)(\omega_g + \delta) + \Gamma_\phi(\omega_g - \delta)(\omega_g + \delta))}. \tag{7.17}$$

At resonance the ratio is $3\Gamma_p/(N\Gamma_m)$. If we choose $\Gamma_p = \frac{N}{3}\Gamma_m$, the two emission rates are equal at resonance. Note that dephasing affects the results only outside the resonance condition.

Figure 7.1 shows the ratio with different dephasing rates as a function of $\frac{\delta}{\sqrt{N}g}$. Dephasing broadens the area where the strong coupling is significant. For larger values of Γ_ϕ the changes in the emission ratio are smaller. This is probably connected to the fact that in our model dephasing causes the stationary state to have molecule superposition states, as discussed in section 6.4.

With negative values of δ the emitted light mainly originates from molecule decay. For positive values of δ SPP decay is dominant. This is reasonable since in the stationary state, due to the excitation into the $|b\rangle$ state, the ρ_{bb} element is the largest. With negative values of δ the bonding hybrid state is closer to the free molecule state while for positive values of δ the bonding state is closer to the free SPP state.

Polarization of the emitted light

In addition to the origin of the emitted light we can look at which external field they were emitted into. We divide the external fields into three parts according to the polarization direction. In the coordinate system where the SPP polarization direction is in the z' direction the system does not emit light that has a polarization vector into the x'-direction, $f_{x'} = 0$. The rate into y-direction is also zero, $f_y = 0$. This is because the only contribution to those directions would come from terms involving the first two integrals of the last equations of (7.6) and (7.8). Those integrals give zero and thus the contribution to x'- and y'-directions is zero.

Into the z'-direction the emission rate is

$$f_{z'} = \left(\Gamma_p + \Gamma_m \frac{N}{3}\right)(\rho_{aa} + \rho_{bb}). \tag{7.18}$$

Since z'-direction is the SPP polarization direction, the emitted light has the same polarization as the SPP.

This is because the only contribution to the other two directions would come from terms involving the first two integrals of the last equations of (7.6) and (7.8). Those integrals give zero and thus the contribution to x'- and y'-directions is zero.

In the natural coordinate system used in section 2, where x- and y-directions are parallel to the surface and the plasmon polarization direction is in the xz-plane $\hat{u}_p = (\sin\beta, 0, \cos\beta)$ the emission rates into x- and z-directions become

$$\begin{aligned} f_x &= \sin^2\beta \left(\Gamma_p + \Gamma_m \frac{N}{3}\right)(\rho_{aa} + \rho_{bb}) \\ f_z &= \cos^2\beta \left(\Gamma_p + \Gamma_m \frac{N}{3}\right)(\rho_{aa} + \rho_{bb}). \end{aligned} \tag{7.19}$$

For s-polarized light the only component the polarization vector has is the y-component. Since the emission rate into y-direction is zero, pure dephasing is not enough to produce s-polarized light.

Symmetrical excitation

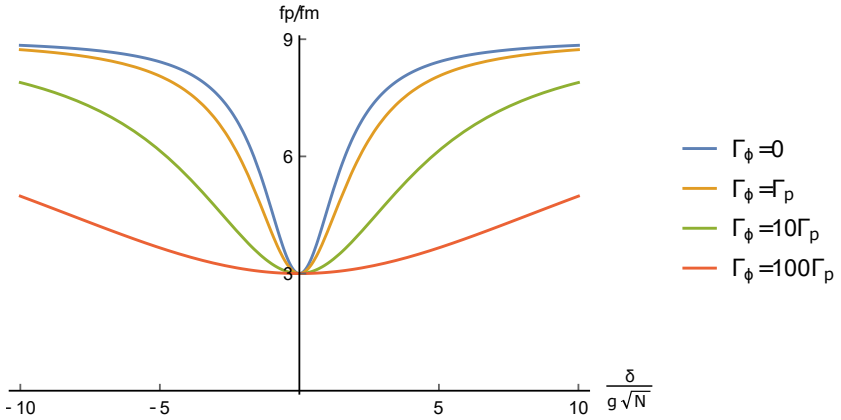

Figure 7.2: Symmetrical excitation case. The ratio between the rate at which SPP decay emits light and the molecule decay emits light as a function of $\delta/\sqrt{N}g$, with different dephasing rates. The SPP decay rate is $\Gamma_p = N\Gamma_m$.

So far we have only considered excitation into the bonding hybrid state $|b\rangle$. We can however modify the model slightly to get a model for excitation symmetrically into both of the hybrid states. Symmetrically here means that half of the photons excite the bonding state and half excite the antibonding state. The only thing we need to do is change the excitation term in the third equation in (7.9) into $\frac{1}{2}\Gamma_{exc}\rho_{00}$ and add the same term into the second equation.

With the symmetrical excitation the ρ_{bb} element in terms of ρ_{aa} becomes

$$\rho_{bb}^{\text{sym}} = \frac{\frac{\Gamma_p}{2}(\omega_g - \delta) + \frac{\Gamma_m}{2}\frac{N}{3}(\omega_g + \delta) + \Gamma_\phi(\omega_g - \delta)(\omega_g + \delta)}{\frac{\Gamma_p}{2}(\omega_g + \delta) + \frac{\Gamma_m}{2}\frac{N}{3}(\omega_g - \delta) + \Gamma_\phi(\omega_g - \delta)(\omega_g + \delta)}\rho_{aa}. \tag{7.20}$$

Now the ratio between the rate of SPP emissions and the rate of molecule emissions becomes in the symmetrical excitation case

$$\frac{f_p^{\text{sym}}}{f_m^{\text{sym}}} = \frac{\Gamma_p(\Gamma_p(\omega_g^2 + \delta^2) + \frac{N}{3}\Gamma_m(\omega_g^2 - \delta^2) + \Gamma_\phi(\omega_g^2 - \delta^2))}{\frac{N}{3}\Gamma_m(\Gamma_p(\omega_g^2 - \delta^2) + \frac{N}{3}\Gamma_m(\omega_g^2 + \delta^2) + \Gamma_\phi(\omega_g^2 - \delta^2))}. \tag{7.21}$$

At resonance the ratio is again $3\Gamma_p/(N\Gamma_m)$. However if we now choose $\Gamma_p = \frac{N}{3}\Gamma_m$ the two emission rates are equal even far from resonance. Thus we choose $\Gamma_p = N\Gamma_m$. Figure 7.2 shows the ratio between the emission rates with different dephasing rates. Because of the symmetrical excitation the ratio is now symmetric with respect to δ. With large values of $|\delta|$ the emission ratio saturates to $\lim_{|\delta|\to\infty} f_p/f_m = 9$. Again increasing the dephasing rate broadens the area in which the coupling is relevant.

7.2 Finding the s-polarization

As discussed in section 7.1.1 pure dephasing alone is not enough to produce emission of s-polarized light. In this section we add a term that allows the emission of s-polarized light.

In section 4.2.3 we construct a decay term for the molecules assuming that they are all coupled to a common external field. In that construction we assume that the correlation length of the photons is infinite so that they can interact with all molecules at the same time. If, however, the correlation length of the photons is finite compared to the correlation length of the molecules, as a first correction we get a term that effectively couples the molecules into separate external fields. This term is the same as the term for the inelastic scattering with phonons, except now the bath is the external photon field and thus the decay rate is different

$$\mathcal{L}_j[\rho] = \Gamma_j \sum_{k=1}^{N} \sum_{\sigma=x,y,z} (\hat{n}_k \cdot \hat{u}_\sigma)^2 (L_k \rho L_k^\dagger - \frac{1}{2}\{L_k^\dagger L_k, \rho\}). \tag{7.22}$$

To simplify the calculation we now disregard dephasing. Adding the correction term leads to the following equations in the stationary state (symmetrical excitation):

$$\begin{aligned}
0 = \dot{\rho}_{00} =& \Gamma_j \sum_m \rho_{mm} - \Gamma_{exc}\rho_{00} + \left(\Gamma_p u_p \frac{\omega_g - \delta}{2\omega_g} + \Gamma_m \frac{N}{3}\frac{\omega_g + \delta}{2\omega_g} + \Gamma_j \frac{\omega_g + \delta}{2\omega_g}\right)\rho_{aa} \\
&+ \left(\Gamma_p u_p \frac{\omega_g + \delta}{2\omega_g} + \Gamma_m \frac{N}{3}\frac{\omega_g - \delta}{2\omega_g} + \Gamma_j \frac{\omega_g - \delta}{2\omega_g}\right)\rho_{bb} \\
0 = \dot{\rho}_{aa} =& -\left(\Gamma_p u_p \frac{\omega_g - \delta}{2\omega_g} + \Gamma_m \frac{N}{3}\frac{\omega_g + \delta}{2\omega_g} + \Gamma_j \frac{\omega_g + \delta}{2\omega_g}\right)\rho_{aa} + \frac{\Gamma_{exc}}{2}\rho_{00} \\
0 = \dot{\rho}_{bb} =& -\left(\Gamma_p u_p \frac{\omega_g + \delta}{2\omega_g} + \Gamma_m \frac{N}{3}\frac{\omega_g - \delta}{2\omega_g} + \Gamma_j \frac{\omega_g - \delta}{2\omega_g}\right)\rho_{bb} + \frac{\Gamma_{exc}}{2}\rho_{00} \\
0 = \dot{\rho}_{nn} =& \Gamma_j \rho_{nn}.
\end{aligned} \tag{7.23}$$

These equations can be easily solved to obtain

$$\begin{aligned}
\rho_{00} =& \frac{2}{\Gamma_{exc}}\left(\Gamma_p u_p \frac{\omega_g - \delta}{2\omega_g} + \Gamma_m \frac{N}{3}\frac{\omega_g + \delta}{2\omega_g} + \Gamma_j \frac{\omega_g + \delta}{2\omega_g}\right)\rho_{aa} \\
\rho_{bb} =& \frac{\Gamma_p(\omega_g - \delta) + \Gamma_m \frac{N}{3}(\omega_g + \delta) + \Gamma_j(\omega_g + \delta)}{\Gamma_p(\omega_g + \delta) + \Gamma_m \frac{N}{3}(\omega_g - \delta) + \Gamma_j(\omega_g - \delta)}\rho_{aa} \\
\rho_{nn} =& 0.
\end{aligned} \tag{7.24}$$

Again ρ_{aa} can be obtained from the trace condition $\mathrm{Tr}(\rho) = \rho_{00} + \rho_{aa} + \rho_{bb} + \sum_n \rho_{nn} = 1$.

Similarly to section 7.1.1 we can look at the polarization of the emitted light. In the natural coordinate system of section 2 the emission rates to the external fields with different

polarizations are

$$\begin{aligned}
f_x =& \left[\sin^2\beta\Gamma_p\frac{\omega_g-\delta}{2\omega_g}+\sin^2\beta\Gamma_m\frac{\omega_g+\delta}{2\omega_g}+\Gamma_j\left(\frac{3}{5}\sin^2\beta+\frac{1}{5}\cos^2\beta\right)\frac{\omega_g+\delta}{2\omega_g}\right]\rho_{aa}\\
&+\left[\sin^2\beta\Gamma_p\frac{\omega_g+\delta}{2\omega_g}+\sin^2\beta\Gamma_m\frac{\omega_g-\delta}{2\omega_g}+\Gamma_j\left(\frac{3}{5}\sin^2\beta+\frac{1}{5}\cos^2\beta\right)\frac{\omega_g-\delta}{2\omega_g}\right]\rho_{bb}\\
&+\Gamma_j\frac{1}{2}\sum_m(1-A_m)\rho_{mm}\\
f_y =& \Gamma_j\frac{1}{5}\frac{\omega_g+\delta}{2\omega_g}\rho_{aa}+\Gamma_j\frac{1}{5}\frac{\omega_g-\delta}{2\omega_g}\rho_{bb}+\Gamma_j\frac{1}{2}\sum_m(1-A_m)\rho_{mm}\\
f_z =& \left[\cos^2\beta\Gamma_p\frac{\omega_g-\delta}{2\omega_g}+\cos^2\beta\Gamma_m\frac{\omega_g+\delta}{2\omega_g}+\Gamma_j\left(\frac{1}{5}\sin^2\beta+\frac{3}{5}\cos^2\beta\right)\frac{\omega_g+\delta}{2\omega_g}\right]\rho_{aa}\\
&+\left[\cos^2\beta\Gamma_p\frac{\omega_g+\delta}{2\omega_g}+\cos^2\beta\Gamma_m\frac{\omega_g-\delta}{2\omega_g}+\Gamma_j\left(\frac{1}{5}\sin^2\beta+\frac{3}{5}\cos^2\beta\right)\frac{\omega_g-\delta}{2\omega_g}\right]\rho_{bb}\\
&+\Gamma_j\sum_m A_m\rho_{mm}.
\end{aligned}\tag{7.25}$$

Now due to the correction term some of the light is emitted with polarization into the y-direction, i.e. some of the light is s-polarized.

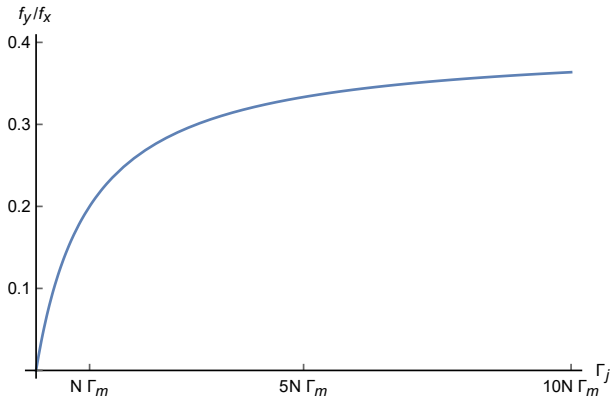

Figure 7.3: Symmetrical excitation case. The ratio between the rate at which light is emitted with polarization into y-direction and with polarization into x-direction as a function of Γ_j at resonance ($\delta = 0$). The SPP decay rate is $\Gamma_p = N\Gamma_m/3$, the SPP polarization angle is $\beta = \pi/3$ and $N = 1\,000\,000$.

At resonance ($\delta = 0$), the ratio between the rates at which light is emitted with polarization into y-direction and with polarization into x-direction is

$$\frac{f_y}{f_x}(\delta=0)=\frac{\Gamma_j}{\sin^2\beta(5\Gamma_p+5\Gamma_m\frac{N}{3}+3\Gamma_j)+\cos^2\beta\Gamma_j}.\tag{7.26}$$

Figure 7.3 shows the ratio as a function of Γ_j. When Γ_j is small compared to the other two rates Γ_p and $\Gamma_m\frac{N}{3}$, the ratio behaves almost linearly. As Γ_j approaches infinity the ratio asymptotically approaches the value

$$\frac{f_y}{f_x}(\delta=0,\Gamma_j\to\infty)=\frac{1}{2\sin^2\beta+1}.\tag{7.27}$$

In the symmetrical excitation case the ratio between the different polarizations decreases as the system leaves resonance. Figure 7.4 shows the ratio as a function of $\frac{\delta}{g\sqrt{N}}$.

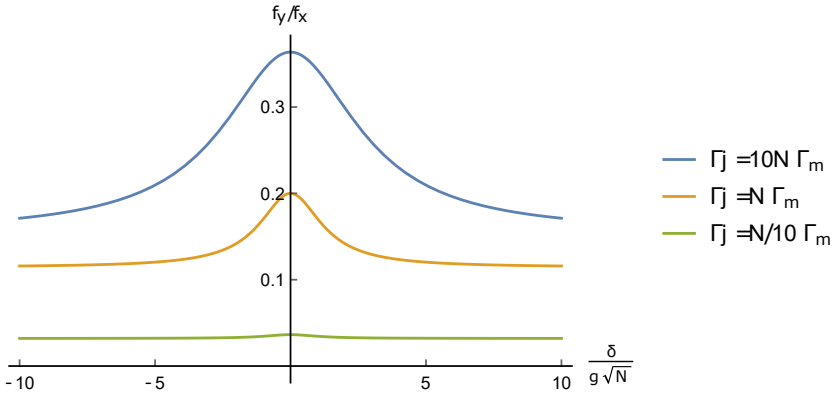

Figure 7.4: Symmetrical excitation case. The ratio between the rate at which light is emitted with polarization into y-direction and with polarization into x-direction as a function of $\delta/\sqrt{N}g$, with different Γ_j. The SPP decay rate is $\Gamma_p = N\Gamma_m/3$, the SPP polarization angle is $\beta = \pi/3$ and $N = 1\,000\,000$.

Excitation into the bonding hybrid state

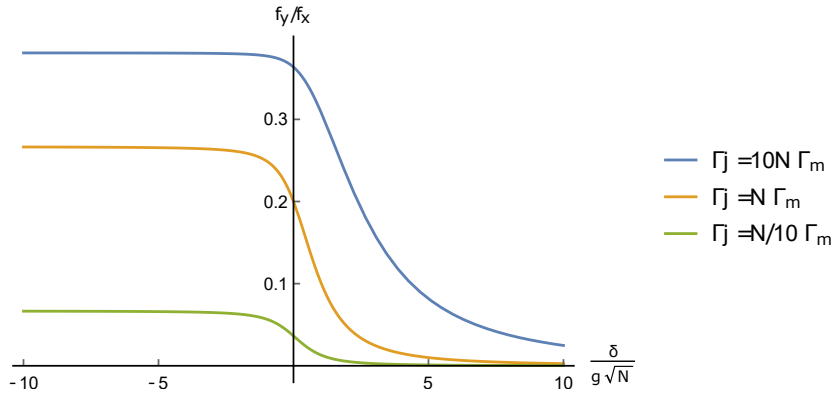

Figure 7.5: Excitation into the bonding hybrid state. The ratio between the rate at which light is emitted with polarization into y-direction and with polarization into x-direction as a function of $\delta/\sqrt{N}g$, with different Γ_j. The SPP decay rate is $\Gamma_p = N\Gamma_m/3$, the SPP polarization angle is $\beta = \pi/3$ and $N = 1\,000\,000$. For excitation into the antibondind state $|a\rangle$ the figure is the same except $\delta \to -\delta$.

If we only excite the bonding hybrid state $|b\rangle$ the ρ_{aa} element vanishes in the stationary state and

$$\rho_{00}^{\text{asym}} = \frac{1}{\Gamma_{exc}}\left(\Gamma_p u_p \frac{\omega_g + \delta}{2\omega_g} + \Gamma_m \frac{N}{3}\frac{\omega_g - \delta}{2\omega_g} + \Gamma_j \frac{\omega_g - \delta}{2\omega_g}\right)\rho_{bb}. \tag{7.28}$$

Now the ratio between the different polarizations becomes

$$\frac{f_y^{\text{asym}}}{f_x^{\text{asym}}} = \frac{\Gamma_j(\omega_g - \delta)}{\sin^2\beta[5\Gamma_p(\omega_g + \delta) + 5\Gamma_m\frac{N}{3}(\omega_g - \delta) + 3\Gamma_j(\omega_g - \delta)] + \cos^2\beta\Gamma_j(\omega_g - \delta)}. \tag{7.29}$$

At resonance the ratio in the asymmetric excitation case is the same as in the symmetrical excitation case. Outside of resonance, however, the behaviour is different.

Figure 7.5 shows the ratio as a function of $\frac{\delta}{g\sqrt{n}}$. For negative values of δ the bonding state behaves like the free molecule states. The molecule states are the origin of the emitted light with polarization into y-direction so it is expected that the ratio for large negative values of δ. For positive values of δ the bonding state behaves less like the free molecule states and more like the SPP state and the system no longer emits light with polarization into y-direction.

The addition of the correction term due to the finite correlation length of the external photon field allows for the emission of s-polarized light. Since the ratio of the emission rates of s-polarized light and the other polarizations is quite small, if Γ_j is smaller than the other process rates Γ_p and $\Gamma_m \frac{N}{3}$, it is possible that the correction term is too small to explain all of the s-polarized light of the experiments. Because of that, further discussion is needed to clarify the microscopical origin of the term and to obtain an analytical formula for the rate Γ_j.

8 Conclusions

Here we provide a summary of the results and discuss ideas for future research on the topic.

We constructed a Lindblad equation for the strongly coupled surface plasmon polariton-molecule system. The Lindblad equation included decay of both the SPP excitation and molecule excitations into external photon fields. For the molecules we included scattering with phonons, inelastic scattering lead to dephasing and inelastic scattering added decay of the molecule excitations. We also added a pumping term to get access to a stationary state. The result is equation (5.8).

We then solved the differential equation numerically in the case of two molecules. The main result of the numerical treatment was that the off-diagonal elements of the stationary density matrix vanish in the eigenbasis when the rates of the dissipation processes are small compared to the coupling inside the system. This was discussed in section 6.2. However, in the case of four molecules we saw that the off-diagonal elements between the molecule superposition states did not vanish in the stationary state. This we attributed to the choice of the molecule superposition eigenstates.

Using the assumption that the off-diagonal elements of the density matrix vanish we proceeded to analytically find the stationary solution of the Lindblad equation. We simplified the treatment by neglecting inelastic scattering with phonons. The main goal of this thesis was to find a dissipation process that would allow for the emission of s-polarized light from the system. In section 7.1 we found that dephasing alone is not enough to create emission of s-polarized light. The light that is emitted from the system with dephasing has the same polarization direction as the SPP.

We were able to find a Lindblad term, equation (7.22) that allows for the emission of s-polarized light. We argued that such a term may arise if we take the correlation length of the external photon field to be finite compared to the correlation length of the molecules. The correction due to the finite correlation length would look like the molecules were coupled to individual external fields.

In section 7.2 we solved the Lindblad equation that includes the correction term but not dephasing. As a result we found that the ratio between s-polarized light and light with polarization into the x-direction increases as the rate Γ_j in the correction term is increased, figure 7.3. For large values of Γ_j the ratio saturates to the value of equation (7.27).

There are three major areas where our treatment could be improved. Firstly when constructing the Lindblad equation we neglected the strong coupling. That makes the construction simple but ultimately wrong. We also assumed that the dissipation processes happen individually. Including the strong coupling and considering the cross terms between the different processes would increase the accuracy of the model and possibly add interesting physics in the cross terms.

Secondly we are not sure that we have chosen the correct molecule superposition eigenstates. We assumed that the off-diagonal elements of the stationary density matrix vanish in the eigenbasis. However, as we saw in the numerical solution for four molecules

the off-diagonal elements between the molecule superposition states did not vanish. To make sure that our assumption is right the molecule superposition eigenstates have to be chosen correctly. This may already be the case for the spherical harmonics basis used in the analytical solution but we have not checked it.

Finally further discussion is needed on the microscopical origin of the correction term (7.22). For experimental testing of our results the process needs to be understood in more detail and an analytical equation for the rate Γ_j is needed. Even tough the correction term allowed the emission of s-polarized light it may be that the term is too small to explain all of the experimental results. In the future other Lindblad terms should also be considered.

Appendix A Spherical harmonics

Spherical harmonics are a solution to the angular part of Laplace's equation in spherical coordinates

$$\nabla_\Omega Y(\Omega) + l(l+1)Y(\Omega) = 0. \tag{A.1}$$

They are defined as

$$Y_l^m(\theta,\phi) = \sqrt{\frac{2l+1}{4\pi}\frac{(l-m)!}{(l+m)!}} P_l^m(\cos\theta) e^{im\phi}, \tag{A.2}$$

where $P_l^m(\cos\theta)$ are the associated Legendre polynomials. The spherical harmonics are normalized according to

$$\int_0^{2\pi} \mathrm{d}\phi \int_0^{\pi} \mathrm{d}\theta \sin\theta Y_l^m(\theta,\phi) Y_{l'}^{m'}(\theta,\phi) = \delta_{ll'}\delta_{mm'}. \tag{A.3}$$

We need only the functions with $m = 0$ and thus we only need the Legendre polynomials with $m = 0$. They are a solution to the Legendre's differential equation

$$\frac{\mathrm{d}}{\mathrm{d}x}\left[(1-x^2)\frac{\mathrm{d}}{\mathrm{d}x}P_l(x)\right] + l(l+1)P_l(x) = 0. \tag{A.4}$$

Legendre polynomials can be defined recursively, the first two polynomials are $P_0(x) = 1$ and $P_1 = x$ and the rest satisfy

$$(l+1)P_{l+1}(x) = (2l+1)xP_l(x) - lP_{l-1}. \tag{A.5}$$

They are orthogonal and normalized according to

$$\int_{-1}^{1} \mathrm{d}x P_k(x) P_l(x) = \frac{2}{2l+1}\delta_{lk}. \tag{A.6}$$

Using the orthogonality we have

$$\int_{-1}^{1} \mathrm{d}x\, xP_l(x) = \int_{-1}^{1} \mathrm{d}x P_1(x) P_l(x) = 0 \tag{A.7}$$

for all $l \in \{0, 2, 3\dots\}$. Another integral we need can be calculated using the recursion relation

$$\begin{aligned}
\int_{-1}^{1} \mathrm{d}x\, x^2 P_l(x)^2 =& \int_{-1}^{1} \mathrm{d}x \frac{1}{(2l+1)^2}((l+1)P_{l+1}(x) + lP_{l-1}(x))^2 \\
=& \frac{(l+1)^2}{(2l+1)^2}\int_{-1}^{1} \mathrm{d}x P_{l+1}(x)^2 + \frac{n^2}{(2n+1)^2}\int_{-1}^{1} \mathrm{d}x P_{l-1}(x)^2 \\
&+ \frac{2l(l+1)}{(2l+1)^2}\int_{-1}^{1} \mathrm{d}x P_{l+1}(x) P_{l-1}(x) \\
=& \frac{2(2l^2+2l-1)}{(2l+3)(2l+1)(2l-1)}
\end{aligned} \tag{A.8}$$

Appendix B Lamb-shift part

Here we go through the details of the Lamb shift in section 4.2.3. The Lamb shift part can be written according to equation (4.27) as

$$[H_{LS}, \rho] = -\sum_{k=l, \epsilon_l = \epsilon_k} \left(\frac{\xi_{Fkl}}{2} [a_k^\dagger a_l, \rho] + \frac{\xi_{Gkl}}{2} [a_k a_l^\dagger, \rho] \right), \tag{B.1}$$

where

$$\begin{aligned} \xi_{Fkl} &= 2P \int \mathrm{d}\omega \frac{g_k(\omega) g_l(\omega)}{(\Omega - \omega)} (N(\omega) + 1) \\ \xi_{Gkl} &= 2P \int \mathrm{d}\omega \frac{g_k(\omega) g_l(\omega)}{(\Omega - \omega)} N(\omega). \end{aligned} \tag{B.2}$$

Using the commutation relation $[a_k, a_l^\dagger] = \delta_{kl}$, plugging in the coefficients ξ_{Fkl} and ξ_{Gkl} and changing the summation indices in the second term gives

$$\begin{aligned} [H_{LS}, \rho] &= -\sum_{k,l} \Bigg(P \int \mathrm{d}\omega \frac{g_k(\omega) g_l(\omega)}{(\Omega - \omega)} (N(\omega) + 1) [a_k^\dagger a_l, \rho] \\ &\qquad + P \int \mathrm{d}\omega \frac{g_k(\omega) g_l(\omega)}{(\Omega - \omega)} N(\omega) ([\delta_{kl}, \rho] - [a_k^\dagger a_l, \rho]) \Bigg) \\ &= -\sum_{k,l} \left(P \int \mathrm{d}\omega \frac{g_k(\omega) g_l(\omega)}{(\Omega - \omega)} [a_k^\dagger a_l, \rho] \right) \\ &= -\sum_{k,l} \Delta_{kl} [a_k^\dagger a_l, \rho], \end{aligned} \tag{B.3}$$

where $\Delta_{lk} = P \int \mathrm{d}\omega \frac{g_k(\omega) g_l(\omega)}{(\Omega - \omega)}$ and the Lamb shift Hamiltonian $H_{LS} = \sum_{kl} \Delta_{lk} a_k^\dagger a_l$ commutes with the system Hamiltonian $H_s = \Omega \sum_j a_j^\dagger a_j$.

The energy shift Δ_{lk} depends on the spectral density $J_{lk}(\omega) = g_l(\omega) g_k(\omega)$. One example of a spectral density is the Lorentz (or Cauchy) distribution

$$J_{lk}(\omega) = \delta_{lk} \frac{I \gamma^2}{(\omega - \Omega)^2 + \gamma^2}, \tag{B.4}$$

where I is the height of the peak of the distribution and γ is the width of the peak. For the Lorentz distribution the energy shift vanishes.

Appendix C Mathematica code for the numerical solution

This code defines the parameters and Hamiltonian for the strong coupling system. The code also solves the eigenbasis of the Hamiltonian and the Lindblad terms are written in the eigenbasis. Then the Lindblad equation is solved with different dissipation processes.

```
ClearAll["Global`*"];
Nm = 4;
g = 1;
a = 0.01;
\[CapitalGamma]exc = a; \[CapitalGamma]p = a; \[CapitalGamma]m = a;
\[CapitalGamma]\[Phi] = a; \[CapitalGamma]j = a;
(*Polar angles of the molecules' polarizations*)
\[Theta]vec = Array[Function[j, (j - 1)*\[Pi]/(Nm - 1)], Nm];
(*Azimuth angles of the molecules' polarizations*)
\[Phi]vec = Array[Function[j, (j - 1)*2*\[Pi]/(Nm - 1)], Nm];
(*Plasmon polarization angle*)
\[Beta] = 0;
G = Array[Function[j, g*Cos[\[Theta]vec[[j]]]], Nm];
\[Delta] = 0.01;
\[Omega] = 10;

(*Polarization vectors*)
u = IdentityMatrix[3]; (*x,y,z-direction vectors*)
up = {Sin[\[Beta]], 0, Cos[\[Beta]]}; (*Plasmon polarization*)
n = Array[Function[j,
    {Sin[\[Theta]vec[[j]]]*Cos[\[Phi]vec[[j]]],
     Sin[\[Theta]vec[[j]]]*Sin[\[Phi]vec[[j]]],
     Cos[\[Theta]vec[[j]]]} ], Nm]; (*Molecule polarizations*)

(*Hamiltonian in the natural basis*)
H0 = ConstantArray[0, {Nm + 2, Nm + 2}];
H0[[1, 1]] = -\[Omega] + \[Delta]/2;
H0[[3 ;; Nm + 2, 2]] = G;
H0[[2, 3 ;; Nm + 2]] = G;
H0[[2, 2]] = -\[Delta]/2;
diagH0 = ConstantArray[\[Delta]/2, Nm];
H1 = ReplacePart[H0, {i_, i_} /; i >= 3 :> diagH0[[i - 2]]];

(*Basis transformation matrix*)
vec = Eigensystem[H1][[2, All]];
```

```
\[Epsilon]mat = Array[Function[j,
     vec[[j, All]]/Sqrt[vec[[j, All]].vec[[j, All]]]], Nm + 2];

(*Hamiltonian in the eigenbasis*)
H = DiagonalMatrix[Eigensystem[H1][[1, All]]];

(*Coherence term*) (*The density matrix will be inserted to X*)
Lcoh[X_?ArrayQ, t_] := I*(X.H - H.X);

(*Plasmon excitation*)(*Exitation to the |b> state*)
b = ConstantArray[0, Nm + 2];
b[[2]] = 1;
Lb = Outer[Times, \[Epsilon]mat[[All, 1]], b\[Conjugate]];
Lbt = Outer[Times, b, \[Epsilon]mat[[All, 1]]];
Lexc[X_?ArrayQ, t_] := \[CapitalGamma]exc*(Lbt.X. Lb
    - 1/2*(Lb.Lbt.X + X.Lb.Lbt));

(*Plasmon relaxation*)
Lp = Outer[Times, \[Epsilon]mat[[All, 1]],
    \[Epsilon]mat[[All, 2]]\[Conjugate]];
Lpt = Outer[Times, \[Epsilon]mat[[All, 2]],
    \[Epsilon]mat[[All, 1]]\[Conjugate]];
Lprel[X_?ArrayQ, t_, dir_] := \[CapitalGamma]p*(up.u[[dir]])^2*
     (Lp.X. Lpt - 1/2*(Lpt.Lp.X + X.Lpt.Lp));

(*Molecule relaxation*)
Lm = Array[Function[j,
    Outer[Times, \[Epsilon]mat[[All, 1]],
      \[Epsilon]mat[[All, j + 2]]\[Conjugate]]], Nm];
Lmt = Array[Function[j,
    Outer[Times, \[Epsilon]mat[[All, j + 2]],
     \[Epsilon]mat[[All, 1]]]], Nm];
l[X_?ArrayQ, t_, j_, k_] :=
    l[X, t, j, k] =
     Lm[[j]].X.Lmt[[k]] - 1/2*(Lmt[[k]].Lm[[j]].X + X.Lmt[[k]].Lm[[j]]);
Lmreljk[X_?ArrayQ, t_, dir_] :=  Array[Function[{j, k},
    (n[[j]].u[[dir]])*(n[[j]].u[[dir]])*l[X, t, j, k]], {Nm, Nm}];
Lmrel[X_?ArrayQ, t_, dir_] := \[CapitalGamma]m *
     Sum[Lmreljk[X, t, dir][[i, j]], {i, Nm}, {j, Nm}];

(*Dephasing*)
P = Array[Function[j,
    Outer[Times, \[Epsilon]mat[[All, j + 2]],
     \[Epsilon]mat[[All, j + 2]]\[Conjugate]]], Nm];
```

```
Pdepj[X_?ArrayQ, t_, j_] := P[[j]].X.P[[j]] - 1/2*(P[[j]].X + X.P[[j]]);
Pdep[X_?ArrayQ, t_] := \[CapitalGamma]\[Phi]*Sum[Pdepj[X, t, j],
    {j, Nm}];

(*Inelastic scattering*)
ljj[X_?ArrayQ, t_, dir_] := Array[Function[j,
    (n[[j]].u[[dir]])*(n[[j]].u[[dir]])*l[X, t, j, j]], Nm];
Lj[X_?ArrayQ, t_, dir_] := \[CapitalGamma]j*
    Sum[Lmreljk[X, t, dir][[i, i]], {i, Nm}];

(*Solutions to the Lindblad equations are found with the DSolve function*)

(*Only relaxation and excitation*)
Clear[\[Rho]matp, \[Rho], funcp, \[Rho]0]; (*Pdep=0,Lj=0*)
funcp[X_?ArrayQ, t_] :=
  Lcoh[X, t] + Lprel[X, t, 1] + Lprel[X, t, 3] + Lmrel[X, t, 1] +
   Lmrel[X, t, 2] + Lmrel[X, t, 3] + Lexc[X, t];
\[Rho]matp[t_] :=
  Array[Subscript[\[Rho], #1 - Nm + 1, #2 - Nm + 1][t] &, {Nm + 2,
    Nm + 2}];
\[Rho]0 = ConstantArray[0, {Nm + 2, Nm + 2}];
\[Rho]0[[2, 2]] = 1;
solp = DSolve[LogicalExpand[
    D[\[Rho]matp[t], t] == funcp[\[Rho]matp[t], t] &&
     \[Rho]matp[0] == \[Rho]0],
   Flatten[\[Rho]matp[t]], t];

(*Relaxation, Excitation and Dephasing*)
Clear[\[Rho]mat, \[Rho], func, \[Rho]0]; (*Lj=0*)
func[X_?ArrayQ, t_] :=
  Pdep[X, t] + Lcoh[X, t] + Lprel[X, t, 1] + Lprel[X, t, 3] +
   Lmrel[X, t, 1] + Lmrel[X, t, 2] + Lmrel[X, t, 3] + Lexc[X, t];
\[Rho]mat[t_] :=
  Array[Subscript[\[Rho], #1 - Nm + 1, #2 - Nm + 1][t] &,
   {Nm + 2, Nm + 2}];
\[Rho]0 = ConstantArray[0, {Nm + 2, Nm + 2}];
\[Rho]0[[2, 2]] = 1;
sol = DSolve[LogicalExpand[
    D[\[Rho]mat[t], t] == func[\[Rho]mat[t], t] &&
     \[Rho]mat[0] == \[Rho]0],
   Flatten[\[Rho]mat[t]], t];

(*Relaxation and Dephasing*)
Clear[\[Rho]mate, \[Rho], funce, \[Rho]0e]; (*Lj=0, Lexc =0*)
funce[X_?ArrayQ, t_] :=
```

```
  Pdep[X, t] + Lcoh[X, t] + Lprel[X, t, 1] + Lprel[X, t, 3] +
   Lmrel[X, t, 1] + Lmrel[X, t, 2] + Lmrel[X, t, 3];
\[Rho]mate[t_] :=
  Array[Subscript[\[Rho], #1 - Nm + 1, #2 - Nm + 1][t] &,
   {Nm + 2, Nm + 2}];
\[Rho]0e = ConstantArray[0, {Nm + 2, Nm + 2}];
\[Rho]0e[[2, 2]] = 1;
sole = DSolve[LogicalExpand[
    D[\[Rho]mate[t], t] == funce[\[Rho]mate[t], t] &&
     \[Rho]mate[0] == \[Rho]0e],
   Flatten[\[Rho]mate[t]], t];

(*Relaxation, Excitation, Dephasing and Inelastic scattering*)
Clear[\[Rho]matj, \[Rho], funcj, \[Rho]0j];
func[X_?ArrayQ, t_] :=
  Pdep[X, t] + Lcoh[X, t] + Lprel[X, t, 1] + Lprel[X, t, 3] +
   Lmrel[X, t, 1] + Lmrel[X, t, 2] + Lmrel[X, t, 3] + Lexc[X, t] +
   Lj[X, t, 1] + Lj[X, t, 2] + Lj[X, t, 3];
\[Rho]matj[t_] :=
  Array[Subscript[\[Rho], #1 - Nm + 1, #2 - Nm + 1][t] &,
   {Nm + 2, Nm + 2}];
\[Rho]0j = ConstantArray[0, {Nm + 2, Nm + 2}];
\[Rho]0j[[2, 2]] = 1;
solj = DSolve[LogicalExpand[
    D[\[Rho]matj[t], t] == func[\[Rho]matj[t], t] &&
     \[Rho]matj[0] == \[Rho]0j],
   Flatten[\[Rho]matj[t]], t];
```

References

[1] S. Enoch and N. Bonod, editors. *Plasmonics : From Basics to Advanced Topics*. Springer Series in Optical Sciences. Springer Berlin Heidelberg, Berlin, Heidelberg, 2012.

[2] P. Törmä and W. L. Barnes. Strong coupling between surface plasmon polaritons and emitters: a review. *Reports on Progress in Physics*, 78(1):013901, 2015.

[3] J. A. Hutchison, T. Schwartz, C. Genet, E. Devaux, and T. W. Ebbesen. Modifying chemical landscapes by coupling to vacuum fields. *Angewandte Chemie International Edition*, 51(7):1592–1596, 2012.

[4] S. Baieva, O. Hakamaa, G. Groenhof, T.T Heikkilä, and J. Toppari. Effect of stokes shift on dynamics of strongly coupled modes between surface plasmon polaritons and photoactive molecules. Submitted to ACS photonics.

[5] A. González-Tudela, P. A. Huidobro, L. Martín-Moreno, C. Tejedor, and F. J. García-Vidal. Theory of strong coupling between quantum emitters and propagating surface plasmons. *Phys. Rev. Lett.*, 110:126801, Mar 2013.

[6] J. del Pino, J. Feist, and F. J. Garcia-Vidal. Quantum theory of collective strong coupling of molecular vibrations with a microcavity mode. *New Journal of Physics*, 17(5):053040, 2015.

[7] I. S. Grant and W. R. Phillips. *Electromagnetism*, volume Manchester physics series. Wiley, 1990.

[8] A. V. Zayats, I. I. Smolyaninov, and A. A. Maradudin. Nano-optics of surface plasmon polaritons. *Physics Reports*, 408(3-4):131–314, 2005.

[9] D. F. Walls and G. J. Milburn. *Quantum Optics*. Springer-Verlag Berlin Heidelberg, 2nd edition, 2010.

[10] B. M. Garraway. The dicke model in quantum optics: Dicke model revisited. *Philosophical Transactions of the Royal Society of London A: Mathematical, Physical and Engineering Sciences*, 369(1939):1137–1155, 2011.

[11] K. Blum. *Density Matrix Theory and Applications*. Springer Series on Atomic, Optical, and Plasma Physics. Springer Berlin Heidelberg, Berlin, Heidelberg, 3rd edition, 2012.

[12] G. Stefanucci and R. van Leeuwen. *Nonequilibrium Many-Body Theory of Quantum Systems: A Modern Introduction*. Cambridge University Press, 2013.

[13] C. A. Brasil, F. F. Fanchini, and R. de Jesus Napolitano. A simple derivation of the Lindblad equation. 2011.

[14] A. Rivas and S. F. Huelga. *Open Quantum Systems: An Introduction*. SpringerBriefs in Physics. Springer Berlin Heidelberg, 2012.

[15] U. Weiss. *Quantum dissipative systems*. Series in modern condensed matter physics. World Scientific, Singapore ; Hackensack, N.J., 4th edition, 2012.

[16] Wolfram Research, Inc. *Mathematica*. Wolfram Research, Inc., Champaign, Illinois, Version 10.4 edition, 2016.

[17] Wolfram language documentation center: Eigensystem. `https://reference.wolfram.com/language/ref/Eigensystem.html`, 2016. Online; accessed 13 Septem-

ber 2016.

[18] Wolfram language documentation center: Dsolve. http://reference.wolfram.com/language/ref/DSolve.html, 2016. Online; accessed 13 September 2016.

[19] Wolfram language documentation center: Machineprecision. http://reference.wolfram.com/language/ref/MachinePrecision.html?q=MachinePrecision, 2003. Online; accessed 13 September 2016.